

Free Heme and Amyloid- β : A Fatal Liaison in Alzheimer's Disease


Elisabeth Chiziane^a, Henriette Telemann^a, Martin Krueger^b, Juliane Adler^a, Jürgen Arnhold^a, A. Alia^{a,c} and Jörg Flemmig^{a,*}

^a*Institute for Medical Physics and Biophysics, Medical Faculty, Leipzig University, Leipzig, Germany*

^b*Institute for Anatomy, Medical Faculty, Leipzig University, Leipzig, Germany*

^c*Leiden Institute of Chemistry, Faculty of Science, Leiden University, Leiden, The Netherlands*

View metadata, citation and similar papers at core.ac.uk

brought to you by  CORE

provided by Leiden University Scholarly Publications

Accepted 10 October 2017

Abstract. While the etiology of Alzheimer's disease (AD) is still unknown, an increased formation of amyloid- β (A β) peptide and oxidative processes are major pathological mechanism of the disease. The interaction of A β with free heme leads to the formation of peroxidase-active A β -heme complexes. However, enzyme-kinetic data and systematic mutational studies are still missing. These aspects were addressed in this study to evaluate the role of A β -heme complexes in AD. The enzyme-kinetic measurements showed peroxidase-specific pH- and H₂O₂-dependencies. In addition, the enzymatic activity of A β -heme complexes constantly increased at higher peptide excess. Moreover, the role of the A β sequence for the named enzymatic activity was tested, depicting human-specific R5, Y10, and H13 as essential amino acids. Also by studying Y10 as an endogenous peroxidase substrate for A β -heme complexes, ratio-specific effects were observed, showing an optimal dityrosine formation at an about 40-fold peptide excess. As dityrosine formation promotes A β fibrillation while free heme disturbs protein aggregation, we also investigated the effect of A β -heme complex-derived peroxidase activity on the formation of A β fibrils. The fluorescence measurements showed a different fibrillation behavior at strong peroxidase activity, leading also to altered fibril morphologies. The latter was detected by electron microscopy. As illustrated by selected *in vivo* measurements on a mouse model of AD, the disease is also characterized by A β -derived microvessel destructions and hemolytic processes. Thus, thrombo-hemorrhagic events are discussed as a source for free heme in brain tissue. In summary, we suggest the formation and enzymatic activity of A β -heme complexes as pathological key features of AD.

Keywords: Alzheimer's disease, A β -heme complexes, amyloid- β fibrillation, amyloid- β toxicity, free heme, hemolysis, peroxidase activity

INTRODUCTION

Alzheimer's disease (AD) is the most common chronic neurodegenerative disease and accounts for about 72% of all elderly patients with cognitive impairment and other symptoms of dementia [1, 2]. The progressive memory deficits and behavioral changes [3] lead to increasing self-care problems of

patients, making AD a major public health problem in Western countries [4, 5]. While the incidence of the disease is clearly associated with increasing age [6, 7], the etiology of sporadic AD, by far the most common form of the disease [8], is still not known [9, 10].

The deposition of the amyloid- β protein precursor (A β PP)-derived peptide amyloid- β (A β) as fibrils was originally regarded mainly as a hallmark for the postmortem identification of the disease [11, 12]. Yet as A β deposition is an early event during AD pathology [7], the peptide is believed to essentially

*Correspondence to: Dr. Jörg Flemmig, Institute for Medical Physics and Biophysics, Medical Faculty, Leipzig University, Härtelstraße 16 – 18, 04107 Leipzig, Germany. Tel.: +49 341 9715772; E-mail: joerg.flemmig@medizin.uni-leipzig.de.

contribute to the neurodegenerative processes [7]. This is clearly illustrated by the fact that point mutations (familial AD) or duplications (Down syndrome) of A β PP, which lead to increased A β formation, cause an early onset of the disease [13]. Animal experiments on the transmissibility of the disease by A β further prove an essential role of the peptide at AD [14].

Biomarkers like oxidized neurotransmitter [15, 16], lipid peroxides [16], and oxidative stress-induced neuron degeneration [16] also suggest a contribution of oxidative processes and reactive oxygen species (ROS) to the AD pathology [17–19]. Yet again the exact mechanisms, e.g., reasons for the elevated ROS formation in the brain of AD patients, are not known [16]. A β is one major target for oxidation during AD [16], leading, for example, to the formation of neurotoxic dityrosine [19–21]. Thereby a mutual promotion of the oxidative activity and A β -derived neurotoxicity seems to exist at AD [16]. In fact, studies on a mouse model of the disease show a local correlation between A β -derived plaque and ROS formation, suggesting A β not only as a target but also as a major source for the elevated oxidative processes at AD [22].

Over 10 years ago, Atamna et al. showed that free heme interacts with A β , leading to the formation of A β -heme complexes, which exhibit a peroxidase activity in the presence of H₂O₂ [23, 24]. The complexes were found to contribute to neurotransmitter degeneration in the brains of patients with AD [19, 20, 24]. Thus, the peroxidase activity of A β -heme complexes may provide a new explanation for the role of both A β and ROS in the pathology of AD. Subsequent studies showed that this peroxidase activity depends on the binding of free heme to histidine (most likely H13) of A β while R5 and Y10 are essential for the subsequent peroxidase activity [19, 25, 26]. Most notably, R5, Y10, and H13 are the only amino acids mutated in murine A β (G5, F10, R13) [20]. Accordingly, mice show a weaker affinity for free heme [2, 26] and exhibit a lower peroxidase activity of A β -heme complexes [19, 26, 27]. These differences may explain the lack of AD-like neuropathy in these animals despite A β fibril formation [19, 20]. The peroxidase activity of A β -heme complexes also leads to peptide dimerization via dityrosine formation (Y10), which promotes A β fibrillation at AD [19, 28, 29]. Yet there are also reports about a delayed A β fibrillation after oxidation [21]. Moreover, free heme is well known to inhibit A β aggregation [19, 30, 31]. This dismantling effect of free heme on A β fibrils

[25] may depend on the interaction of the heme group with the hydrophobic part of the peptide (F19, F20) [26, 32]. Thus, the influence of A β -heme complex-derived peroxidase activity on the plaque formation in AD is still not clear.

In the current study, we carefully reinvestigated the peroxidase activity of A β -heme complexes, thereby focusing on aspects not considered before. By applying non-aggregating A β _{1–16} [25], we observed higher enzymatic activities with increasing peptide-heme ratios as well as at higher H₂O₂ concentrations and decreasing pH values. By performing mutational studies, we also systematically tested the influence of the peptide sequence on the peroxidase activity of A β -heme complexes, showing the importance of the human-specific amino acids R5, Y10, and H13. Furthermore, the named tyrosine residue was confirmed to represent a major endogenous substrate for the peroxidase activity of A β -heme complexes.

Dityrosine may promote the A β fibrillation [21] while free heme has an inhibitory effect on the formation of the peptide fibrils [33]. Thus, we also investigated the effect of H₂O₂ and/or free heme on the fibrillation of A β _{1–40}. These studies showed delayed fibrillation kinetics of the peptide in the presence of peroxidase components, which means a prolonged existence of potentially neurotoxic A β oligomers [21, 34].

Finally, we also performed *in vivo* studies on a mouse model for AD, thereby focusing on A β -derived blood flow alterations and the deposition of the peptide at cerebral vessel walls. Further investigations showed the co-localization of A β and free iron in the brain tissue of Tg2576 mice. Based on these results we suggest A β -derived microhemorrhages (cerebral amyloid angiopathy, CAA) and hemolytic events induced by this peptide as potential mechanisms for the accumulation of free heme in the brain tissue of AD patients. Accordingly, A β -heme complexes are discussed as possible key contributors to the pathology of this neurological disease.

MATERIALS AND METHODS

General

Most experiments were performed in 10 mM phosphate buffered saline (PBS, Sigma-Aldrich, Steinheim, Deutschland), pH 7.4. For measurements at pH 6.5 a citrate-phosphate buffer (CPB) prepared

from 10 mM citrate (Merck, Darmstadt, Germany), 20 mM disodium hydrogen phosphate, and 140 mM NaCl (both Sigma-Aldrich, Steinheim, Germany) was used. Hemin (chloride salt of ferric protoporphyrin IX, Sigma Aldrich, Steinheim, Germany) as a model for free heme was freshly prepared on a daily basis as a 10 mM stock solution in 0.1 M NaOH [24, 35].

A β with the human-specific sequence was obtained from Rockland, Limerick, PA, USA (A β ₁₋₁₆) or AlexoTech, Umeå, Sweden (A β ₁₋₄₀). Selected mutants and the rodent variant of A β ₁₋₁₆ were synthesized in the Core unit DNA technologies of the IZKF Leipzig (Interdisziplinäres Zentrum für Klinische Forschung, Interdisciplinary Center for Clinical Research), Medical Faculty, University Leipzig, Leipzig, Germany. Stock solutions (500 μ M) of A β were prepared in PBS (A β ₁₋₁₆) or 10 mM borax buffer, pH 9.0 (A β ₁₋₄₀) and stored at -20°C until usage. The latter buffer was prepared by supplementing sodium borate (Sigma-Aldrich, Steinheim, Germany) with 140 mM NaCl and adjusting the pH value with 0.1 mM NaOH (Honeywell, Seelze, Germany).

Peroxidase activity

The peroxidase activity of A β -heme complexes was quantified by performing 2,2'-azino-bis(3-ethylbenzothiazoline-6-sulfonic acid)- (ABTS-) based absorbance measurements [19, 36] in a plate reader (TECAN Infinite M200, Männedorf, Switzerland): Briefly, the non-aggregating A β ₁₋₁₆ [25] (1–160 μ M) was pre-incubated for 5 min [37] with hemin (1–10 μ M) and ABTS (1 mM, Sigma-Aldrich, Steinheim, Germany) in PBS (pH 7.4) or CPB (pH 6.5) at 37°C by using 96-well plates. After H₂O₂ (Sigma-Aldrich, Steinheim, Germany) addition (usually 500 μ M) via an injector device the formation of ABTS radical cations (ABTS^{•+}) was followed spectroscopically at 734 nm ($\epsilon_{734} = 1.5 \times 10^4 \text{ M}^{-1} \text{ cm}^{-1}$) [36, 38] for up to 90 min. All given concentrations are final ones. From the observed initial slope of the absorbance increase the peroxidase activity was determined and expressed as mU/ml [39].

The H₂O₂ stock solution used for the initiation of the peroxidase activity was freshly prepared from a 30 % stock solution by diluting in bidistilled H₂O, determined spectroscopically at 230 and 240 nm ($\epsilon_{240} = 74 \text{ M}^{-1} \text{ cm}^{-1}$, $\epsilon_{230} = 43.6 \text{ M}^{-1} \text{ cm}^{-1}$) and stored at 4°C till injection [40, 41]. In some experiments, instead of H₂O₂ injection a

glucose/glucose oxidase-system (G/GO-system) was applied for a constant hydrogen peroxide generation. Thereby 10 mM glucose and 2–200 mU/ml GO were used to realize different H₂O₂ production rates.

Dityrosine formation

The peroxidase activity of A β -heme complexes was also measured by following the formation of dityrosine bridges from the human-specific Y10 residue [25]. Briefly, 100 μ M of the A β ₁₋₁₆ peptide were pre-incubated with hemin (0.1–100 μ M) at 37°C. After H₂O₂ injection (usually 500 μ M) the formation of dityrosine was followed for up to 90 min via fluorescence measurements (excitation: 320 nm, emission: 410 nm) [19, 21, 42] by using the TECAN plate reader. Again in some experiments, the G/GO-system was used instead of H₂O₂ injection. Moreover, in selected samples 1 μ M horseradish peroxidase (HRP, Sigma-Aldrich, Steinheim, Germany) was added instead of hemin [21].

The formation of dityrosine due to the peroxidase activity of A β -heme complexes was also verified by using matrix-assisted laser desorption/ionization time-of-flight (MALDI-TOF) mass spectrometry. Briefly, 100 μ M A β ₁₋₁₆ were incubated with up to 2 μ M hemin or 1 μ M HRP. Then 100 μ M H₂O₂ were added and the samples were incubated for 20 h at 37°C. Afterwards 4 μ M hemopexin (Hpx) was applied to bind hemin. The samples were subsequently centrifuged through a filter with 30 kDa cut-off to remove both Hpx-hemin complexes and HRP. Then 0.5 M 2,5-dihydroxybenzoic acid (DHB, Sigma-Aldrich, Steinheim, Germany) in methanol supplied with 0.1% trifluoroacetic acid (TFA, Sigma-Aldrich, Steinheim, Germany) was added as a matrix and the samples were analyzed in the positive mode of a Bruker Autoflex (Bruker Daltonics GmbH, Leipzig, Germany) mass spectrometer equipped with a 337 nm nitrogen laser [43].

Amyloid- β fibrillation

The aggregation of A β ₁₋₄₀ was followed by using Thioflavin T (ThT, Sigma-Aldrich, Steinheim, Germany) [44]. Briefly, the integration of ThT into the peptide fibrils was followed for about 72 h at 37°C by performing fluorescence measurements (excitation: 440 nm, emission: 485 nm) [32, 44] in the TECAN plate reader. While 50 μ M A β and 20 μ M ThT were used throughout [45], in selected experiments heme (up to 10 μ M), HRP (1 μ M) and/or H₂O₂ (500 μ M)

were added. The peptide was pre-incubated with heme, HRP, and/or H_2O_2 for 4 h at $37^\circ C$. Afterwards ThT was added and the formation of $A\beta$ fibrils was followed at $37^\circ C$ for up to 96 h. Thereby the fluorescence intensities of the samples were measured every 30 min after shaking the 96-well plate for 10 s.

For each condition the obtained values were corrected for the fluorescence intensities observed in the absence of $A\beta_{1-40}$ [45]. By fitting the curves to a sigmoidal function (equation 1) the fibrillation half-time ($t_{1/2}$, corresponds to h) and the apparent fibrillation rate constant (k_{obs} , corresponds to $1/\tau$) were determined [32, 46, 47]. If no sigmoidal fitting was possible a hyperbolic fitting function (equation 2) was applied to determine $t_{1/2}$ and k_{obs} .

$$y = (F_1 + m_1x) + \frac{(F_2 + m_2x)}{1 + e^{-\frac{x-h}{\tau}}} \quad (1)$$

$$y = \frac{F_1 - F_2}{1 + e^{-\frac{x-h}{\tau}}} + F_2 + m_2x \quad (2)$$

The formation of $A\beta$ fibrils was verified by using scanning transmission electron microscopy (STEM) [31, 32]. Briefly, 10 d after the ThT measurements $1 \mu l$ of selected samples were applied on formvar coated copper grids, dried for 2 h and negatively stained with 1% uranyl acetate [14]. STEM was performed on a Zeiss SIGMA electron microscope (Zeiss, Jena, Germany) equipped with a STEM detector and ATLAS software. From the STEM pictures the morphology was analyzed [11].

In vivo measurements

For the *in vivo* investigation, Tg2576 mice, which contain human $A\beta$ PP with the Swedish double mutation (K670N, M671L) under control of a hamster prion protein promoter [48], were used. Age-matched (18 months) non-transgenic littermates served as control mice. All animal experiments were conducted at Leiden University after being approved by the Institutional Animal Care and Use Committee in accordance with the NIH Guide for the care and use of laboratory animals.

Magnetic resonance angiography (MRA) measurements were conducted on a vertical wide-bore 17.6 T Bruker spectrometer (Bruker BioSpin GmbH, Rheinstetten, Germany) with a 1000 mTm^{-1} actively shielded imaging gradient insert. A birdcage radio-frequency coil with an inner diameter of 2 cm was used. The system was interfaced to a PC

running Topspin 2.0 and Paravision 5.0 software. Time-of-flight angiograms were obtained by using a three-dimensional gradient-echo sequence and generation of maximum-intensity projections [49].

Histological analysis for the identification of $A\beta$ deposits, CAA and iron was performed as described previously [49, 50]: First, mice were anesthetized and transcardially perfused with PBS, pH 7.4, followed by 4% buffered paraformaldehyde (ThermoShandon, Runcorn, UK) through the left cardiac ventricle. Afterwards the brain was dissected out, placed in the same fixative for 48 h, dehydrated, and embedded in paraffin. Subsequently $5 \mu m$ coronal sections were cut using a vibratome.

To detect $A\beta$, brain sections were subjected to immunohistochemistry using anti- $A\beta$ (6E10) or anti- $A\beta_{1-40}$ (BC40) antibodies. Immuno-labeling was visualized by using the Vectastain ABC kit (Vector laboratories, Bulingame, UK) according to the manufacturer's instructions. $A\beta$ -associated redox-active iron was detected histochemically as described previously [51, 52]. Briefly, the brain sections were incubated in 7% potassium ferrocyanide in 3% HCl solution for 15 h and subsequently incubated in 3.5 mM 3,3'-diaminobenzidine (DAB) and 4.4 mM H_2O_2 for 10 min. Images of the histological sections were obtained using a Leica DM RE HC microscope, interfaced to a Leica DC500 3CCD digital camera (both Leica Microsystems GmbH, Wetzlar, Germany).

Statistics

All ABTS-based kinetic measurements were performed in triplicate. The peroxidase activity was calculated from the initial slope of the averaged kinetic curve whereby the given standard deviations correspond to the coefficient of determination for the applied linear curve fit. Also the fluorescence measurements for the determination of dityrosine formation were performed in triplicate and an average curve was created. From the stable fluorescence plateau, the amount of dityrosine was determined whereby the given standard deviation corresponds to the oscillations of the fluorescence values within this time frame. The MALDI-TOF measurements for the verification of dityrosine were performed in triplicate and mean and standard deviation of the relative peak intensities were calculated.

For the aggregation measurements with ThT, again at least three independent experiments were performed. The obtained kinetic curves were averaged,

corrected, and fitted to a sigmoidal or hyperbolic curve to determine $t_{1/2}$ and k_{obs} . The standard deviation given for these values corresponds to the coefficient of determination obtained during the curve fit. The average fibril diameter was determined by analyzing the microscopic pictures. Thereby in each sample ten randomly chosen fibrils were measured to calculate mean and standard deviation of the fibril diameter.

For all results, significant differences were determined by using a Student's two tailed t -test after verifying the Gaussian distribution of the data (Shapiro-Wilk test). Thereby weakly significant ($*p \leq 0.05$), significant ($**p \leq 0.01$), or strongly significant ($***p \leq 0.001$) differences were determined.

The presented results from the MRA measurements and the microscopic analysis of the brain sections are representative examples obtained during the analysis of multiple measurements. Five Tg2576 and five control mice were used for the *in vivo* studies.

RESULTS

Heme peroxidase activity promotion by A β

Using ABTS-based kinetic measurements with A β_{1-16} we observed a clear enhancement of the heme-derived peroxidase activity in the presence of the peptide. Furthermore, the peroxidase activity of A β -heme complexes showed a characteristic pH- and H $_2$ O $_2$ -dependence. As illustrated by the representative kinetic curves shown in Fig. 1A, while free heme (10 μ M, grey dashed line) led only to a minor and slow formation of ABTS $^{\bullet-}$, in the presence of increasing A β concentrations (10–180 μ M, grey - black lines) constantly elevating ABTS oxidation rates were observed. In fact, as shown in Fig. 1B in the presence of 2 μ M peptide already a strongly significant elevated peroxidase activity (1.18 ± 0.01 mU/ml) was observed as compared to the heme control (1.03 ± 0.01 mU/ml). With increasing A β -heme ratio an almost linear increase in the

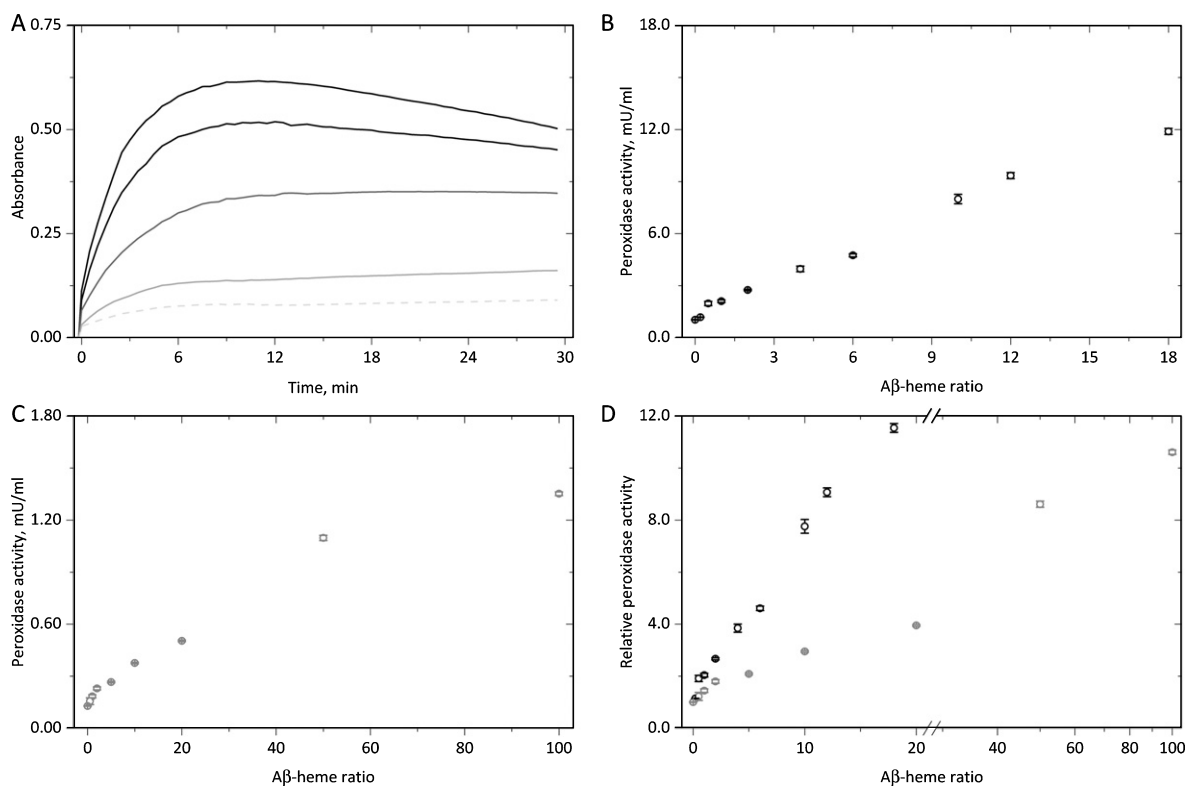


Fig. 1. A β -derived acceleration of heme-dependent peroxidase activity. 10 μ M heme and up to 180 μ M A β_{1-16} (A and B) or 1 μ M heme and up to 100 μ M A β_{1-16} (C) were pre-incubated in PBS in the presence of ABTS. After H $_2$ O $_2$ addition (500 μ M), the formation of ABTS $^{\bullet-}$ was followed spectroscopically. While in (A) kinetic samples for 10 μ M heme alone (grey, dashed) or in the presence of 10 μ M, 60 μ M, 120 μ M, or 180 μ M peptide (grey to black lines) are shown, in (B) the peroxidase activity calculated from the initial slopes is plotted against the A β -heme ratio. The corresponding data for 1 μ M heme and up to 100 μ M A β are displayed in (C). In (D) the relative A β -derived promotion of the heme-dependent peroxidase activity is shown for both conditions.

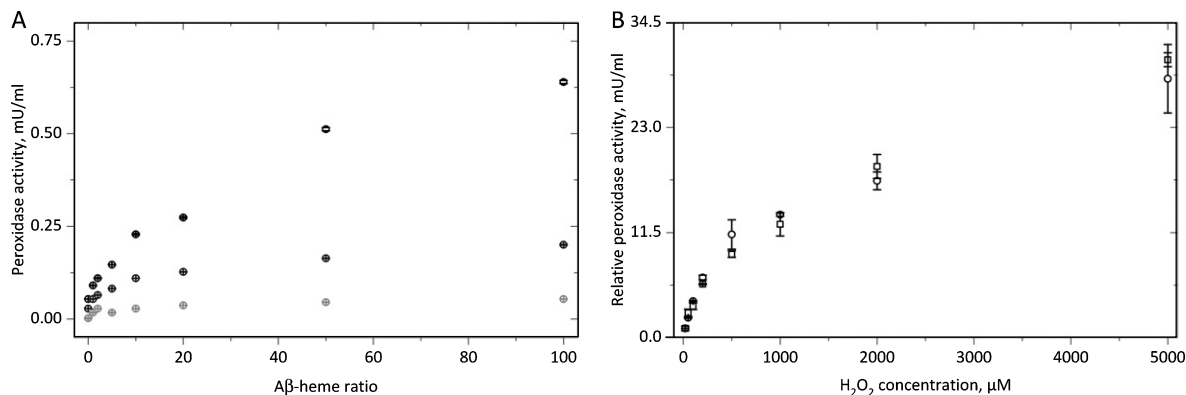


Fig. 2. Effect of A β on the H₂O₂-dependent heme peroxidase activity. In (A) 1 μ M heme and up to 100 μ M A β ₁₋₁₆ were pre-incubated in PBS in the presence of ABTS and 2 mU/ml (light grey), 20 mU/ml (grey) or 200 mU/ml GO (black). After addition of 10 mM glucose the formation of ABTS^{•-} was followed and the initial peroxidase activity determined. In (B) for 10 μ M heme (squares) or 1 μ M heme/10 μ M A β ₁₋₁₆ (circles) the ABTS oxidation was followed after addition of 20–5000 μ M H₂O₂. The calculated initial peroxidase activities were related to the particular values observed at 20 μ M H₂O₂.

peroxidase activity was observed with the highest value (11.89 ± 0.18 mU/ml) at 18-fold peptide excess over heme. Yet as illustrated by the data obtained from measurements with 1 μ M heme (peroxidase activity: 0.13 ± 0.00 mU/ml) and up to 100 μ M peptide (Fig. 1C) at even higher A β -heme ratios a saturating effect can be observed. In the absence of heme, the peptide exhibited no peroxidase activity (not shown).

Most interestingly, by plotting the relative increase in the peroxidase activity (referred to the value obtained in the sole presence of heme) against the A β -heme ratio (Fig. 1D) for the experiments with 10 μ M heme (black), an approximate 12-fold increase in the peroxidase activity was already observed at an 18-fold peptide excess. In contrast, by using 1 μ M heme (grey), a comparable effect was only observed in the presence of a 100-fold peptide excess. At a 10-fold excess of A β ₁₋₁₆, a 7.8-fold higher peroxidase activity was found for 10 μ M heme while with 1 μ M heme, a 10-fold peptide excess led only to an about 2.9-fold higher peroxidase activity.

As shown in Supplementary Figure 1, we also performed measurements at pH 6.5. As illustrated by the displayed selected kinetic curves (Supplementary Figure 1A) and proofed by determining the corresponding activities the peroxidase activity of 10 μ M heme (1.96 ± 0.09 mU/ml) was already about 90% higher as compared to the value observed at pH 7.4. Also upon application of increasing peptide concentrations (Supplementary Figure 1B), higher peroxidase activities were observed at pH 6.5 (black) than at pH 7.4 (white). Yet the peptide-dependent pro-

motion of the heme-derived peroxidase activity was not completely equal for both pH values: While at pH 7.4, an 18-fold peptide excess led to an almost 12-fold increase in the peroxidase activity (see also Fig. 1D); at pH 6.5, a A β -heme ratio of 18:1 led only to an about 7.8-fold higher ABTS^{•-} formation rate.

Instead of a H₂O₂ bolus addition, we used the glucose/glucose oxidase-system (G/GO-system) in selected experiments in order to create a constant hydrogen peroxide production during the peroxidase measurements. As shown in Fig. 2A, for all applied GO concentrations (2–200 mU/ml) again a clear A β -heme ratio-dependent increase in the peroxidase formation rate was observed. Thereby a minor H₂O₂ dependence can be observed: At 200 mU/ml GO (black) an A β -heme ratio of 100/1 instead of 1/1 led to an about 7.0-fold higher peroxidase activity. However, by using 20 mU/ml (grey) or 2 mU/ml (light grey) GO, a comparison of the named A β -heme ratios showed only an about 3.7-fold or 3.2-fold increase in the ABTS^{•-} production rate. As calculated from a calibration curve (Supplementary Figure 2), the used amount of GO yields to a constant production of 2.62 μ M, 25.69 μ M, or 159.05 μ M H₂O₂/min, respectively, which meets the expected H₂O₂ production rates.

Yet, as illustrated in Fig. 2B, by incubating either 10 μ M heme (squares) or 10 μ M A β and 1 μ M heme (circles) with increasing H₂O₂ concentrations the increase in the relative peroxidase activity (referred to the values obtained at 20 μ M H₂O₂) was almost equal: For instance, the application of 500 μ M H₂O₂ led to an 11.3-fold higher activity in the case

of the A β -heme complex while for heme alone a 9.1-fold increase was observed. These results proof again the heme-based enzymatic activity of A β -heme complexes. Still, again a minor effect of the peptide on the H₂O₂ concentration-dependent promotion of the heme-derived peroxidase activity may be guessed.

A β sequence-dependent heme peroxidase activity promotion

Next we tested the relevance of the human-specific amino acid sequence of A β for the promotion of the heme-dependent peroxidase activity by incubating 10 μ M heme with a 10-fold excess of different A β peptides. Thereby we focused on sequence differences between the human and rodent peptide, but also included selected mutants described in the literature. The results clearly show that the enzymatic activity of A β -heme complexes strongly depends on the human-specific sequence of the peptide.

As illustrated by the representative kinetic curves in Fig. 3A, the exchange of one of the three human-specific amino acids of A β ₁₋₁₆ (R5, Y10, H13) to the rodent equivalent (G5, F10, R13) already led to considerably lower curves in comparison to the human peptide (black line). Yet the ABTS^{•-} formation of these single mutants (dark grey lines) seems to be still stronger in comparison to the mouse peptide (light grey line) and certainly stronger than the peroxidase activity of heme alone (light grey dashed line). As shown by the exemplary curves in Fig. 3B, the corresponding double mutants (R5G, H13R; R5G, Y10F; Y10F, H13R) (grey lines) apparently showed an even lower peroxidase activity than the single mutants that was, however, still higher than the ABTS oxidation rate of the mouse peptide (light grey line). As both the human and the rodent A β peptide contain a histidine at position 14, an artificial double mutant was also included where both the human-specific H13 and H14 were replaced by glycine. This double mutant seemed to show an even lower peroxidase activity than the mouse peptide, which was, however, still stronger than the value observed for heme alone (light grey dashed line).

In Fig. 3C, the peroxidase activity for all samples determined from the initial slope is shown. While for heme alone, a peroxidase activity of 1.03 ± 0.01 mU/ml was found, the peroxidase activity in the presence of a 10-fold excess of human A β was about 8-fold higher (7.99 ± 0.27 mU/ml). In contrast by using rodent A β , only an about 2.5-fold higher value (2.49 ± 0.01 mU/ml) was observed. Upon mutation

of one of the human-specific amino acids in A β ₁₋₁₆ with the rodent equivalent significant (R5G) or highly significant (Y10F, H13R) lower peroxidase activities were observed as compared to the human peptide. By using single mutants described in the literature (R5N, Y10G, H13A), again a highly significant reduction of the A β -mediated promotion of the heme-dependent peroxidase activity was found. In fact, the effect of these single mutants was always stronger as compared to the corresponding rodent mutations (see, for example, Y10F and Y10G). However, all tested single mutants still led to a strongly significant higher peroxidase activity than the rodent A β peptide.

The peptides where two of the three human-specific amino acids were replaced by the rodent equivalents (R5G, Y10F; R5G, H13R; Y10F, H13R) had even lower promoting effects on the heme-derived peroxidase activity. Still the obtained values were strongly significant higher than by using the rodent peptide. Since both in the human and the rodent A β sequence a histidine residue is present at position 14 of the peptide, we guessed that a mutation of the human-specific histidine 13 might be counterbalanced by H14. In fact, by applying a corresponding double mutant (H13G, H14G), the obtained peroxidase activity (2.06 ± 0.03 mU/ml) was strongly significantly lower than for the rodent peptide. All tested peptides exhibited no peroxidase activity in the absence of heme (not shown).

Y10 as an endogenous peroxidase substrate of A β -heme complexes

By measuring the formation of dityrosine bridges, the human-specific Y10 in the human peptide was found as an important endogenous substrate for the peroxidase activity of A β -heme complexes. Thereby the efficiency of dityrosine formation depended on the A β -heme ratio, the H₂O₂ concentration, and the A β sequence. The peroxidase-derived formation of human A β dimers due to Y10-dependent dityrosine formation was also verified by MALDI-TOF mass spectrometry.

In Fig. 4A representative kinetic curves illustrate the fluorescence increase at 410 nm (excitation: 320 nm) after the addition of 500 μ M H₂O₂ to 100 μ M A β ₁₋₁₆ in the presence of different heme concentrations. While at an A β -heme ratio of 10:1 (10 μ M heme, black), almost no fluorescence increase was observed; at 2.25 μ M heme (grey, A β -heme ratio: 44.4:1), a fast and strong increase in the

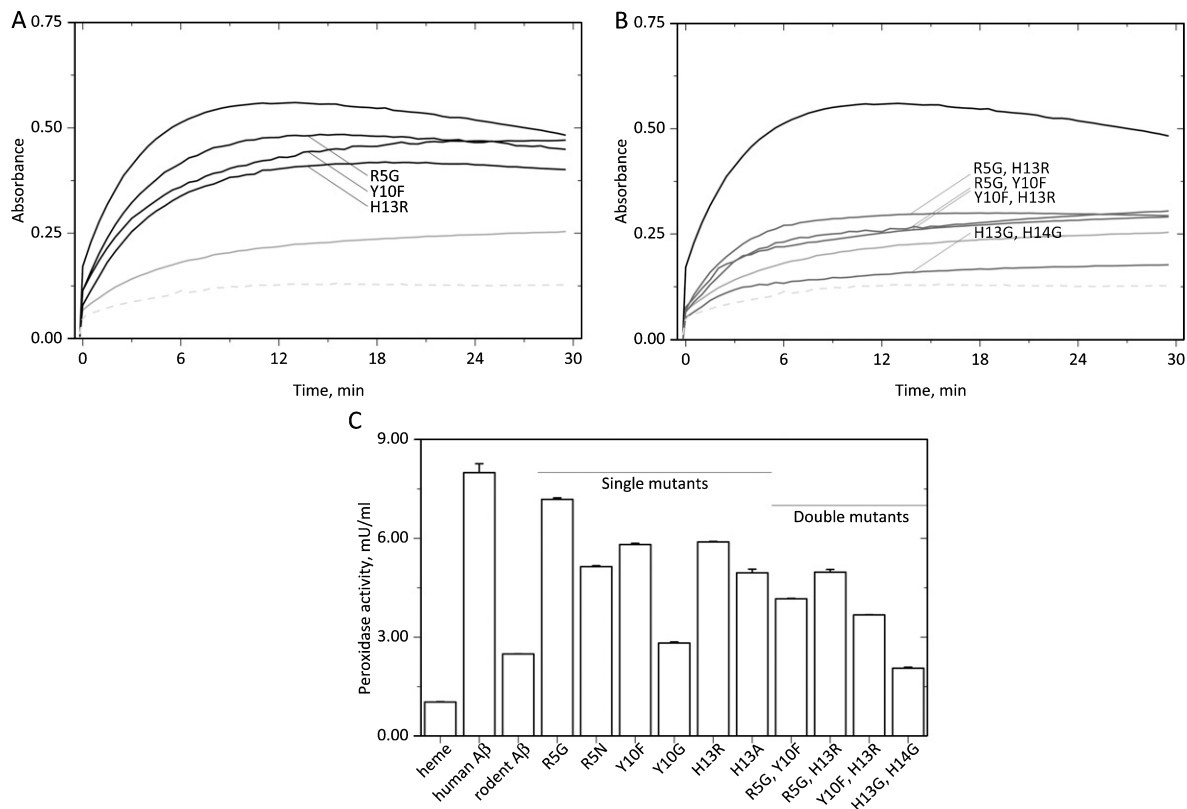


Fig. 3. A β sequence-dependent acceleration of the heme-derived peroxidase activity. 10 μ M heme alone or in the presence of 100 μ M A β were pre-incubated in PBS in the presence of ABTS. After H₂O₂ addition (500 μ M) the formation of ABTS^{•-} was followed spectroscopically. Both in (A) and (B) kinetic sample spectra for heme alone (light grey, dashed) or in the presence of the human (black line) or the rodent (grey line) peptide are shown. Also kinetic examples for peptides with one (A) or two (B) mutations of the human-specific amino acids R5, Y10, and H13 are included. In (C) for all tested peptides the peroxidase activity calculated from the initial ABTS^{•-}-derived absorbance increase are shown. Thereby also values obtained for single mutants of human A β ₁₋₁₆ described in the literature are included.

fluorescence at 410 nm took place, indicating a quick formation of dityrosine bridges. However, at even higher A β -heme ratios (e.g., 200:1, light grey), again lower fluorescence values were observed, showing a lower yield of dityrosine. In the sole presence of the peptide (dashed line), no dityrosine formation took place.

By using the data obtained from control measurements with HRP (not shown), the displayed maximal fluorescence values at 410 nm were translated to the amount of dityrosine formed after H₂O₂ addition. The corresponding data for the measurements in the presence of 500 μ M H₂O₂ (black) and 100 μ M H₂O₂ (white) are shown in Fig. 4B. For 500 μ M H₂O₂, starting at an A β -heme ratio of 12.5:1 (corresponds to 8 μ M heme) up to an A β -heme ratio of 133.3:1 (0.75 μ M heme) significant higher fluorescence values as compared to the negative control (only peptide, dashed line) were observed. Thereby the highest dity-

rosine formation was found at an A β -heme ratio of 44.4:1. The determined 21.08 ± 2.02 μ M dityrosine correspond to a relative yield of 42.2%, given the application of 100 μ M peptide. In the presence of 100 μ M H₂O₂, a comparable ratio dependence was observed. Under these conditions, the highest dityrosine formation was found at an A β -heme ratio of 33.3:1 (13.37 ± 1.80 μ M, 26.7% relative yield).

As shown in Fig. 4C, by using 10 mM glucose and glucose oxidase (black: 200 mU/ml, grey: 20 mU/ml, white: 2 mU/ml) as a H₂O₂-generating system an optimal dityrosine formation was always observed in the presence of 2.25 μ M heme, which corresponds to an A β -heme ratio of 44.4:1. Moreover, the results from the measurements with the G/GO-system confirm the observation that in the presence of more H₂O₂ higher dityrosine yields are obtained although the values observed at 200 mU/ml GO (10.30 ± 1.49 μ M, 20.6 % relative yield) and 2

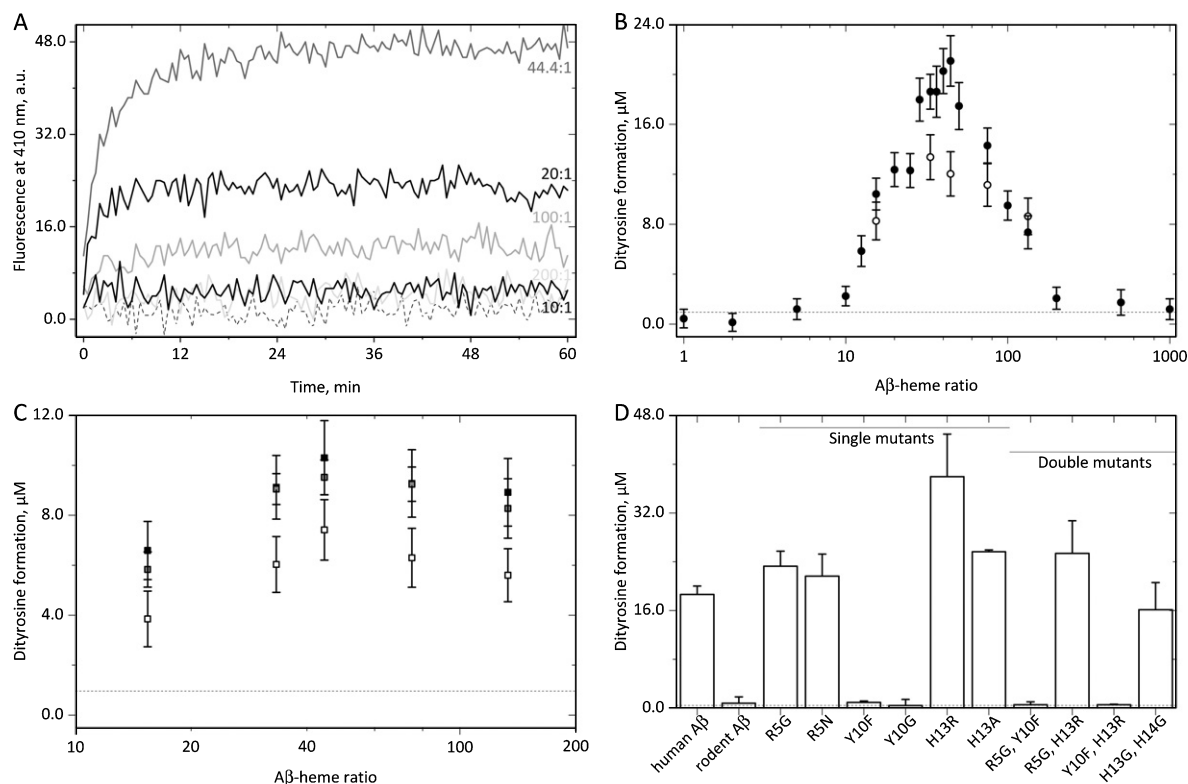


Fig. 4. Formation of dityrosine bridges due to heme-derived peroxidase activity. The formation of dityrosine was quantified by following the increase in the fluorescence at 410 nm (excitation: 320 nm) after adding up to 500 μM H_2O_2 to 100 μM $\text{A}\beta_{1-16}$ in the presence of different heme concentrations. As illustrated for 500 μM H_2O_2 in (A) and quantified for 500 μM (black) and 100 μM (white) H_2O_2 in (B) at an $\text{A}\beta$ -heme ratio of about 30-50:1 an optimal dityrosine formation was observed. Comparable results were obtained by using the G/GO-system (C). Upon application of single and double mutants of human $\text{A}\beta_{1-16}$ (D) a dityrosine formation was never observed in the absence of Y10. In the presence of the named amino acid a fairly comparable dityrosine formation rate was found for all tested peptides.

mU/ml GO ($7.42 \pm 1.21 \mu\text{M}$, 14.8% relative yield) showed no significant difference.

We also tested the dityrosine formation from rodent $\text{A}\beta$ as well as the single and double mutants of human $\text{A}\beta$ mentioned before (see above) by incubating the peptides (100 μM) with 3 μM heme in the presence of 500 μM H_2O_2 . As illustrated by the quantitative analysis of the obtained data (Fig. 4D), all Y10-containing peptides showed a comparable dityrosine formation. For the R5G mutant, weakly significant higher final fluorescence values were seen, while for H13R and H13A, significant higher final fluorescence values were obtained, suggesting bigger dityrosine yields for these peptides. In fact, while the obtained fluorescence value for human $\text{A}\beta_{1-16}$ at the given $\text{A}\beta$ -heme ratio (33.3:1) was $18.62 \pm 1.39 \mu\text{M}$ dityrosine, for H13R, an about 2-fold higher yield ($37.97 \pm 6.99 \mu\text{M}$ dityrosine) was calculated. Most interestingly for the artificial histidine double mutant (H13G, H14G), no significant

reduction in the dityrosine yield was observed despite the strongly significant lower peroxidase activity observed in the corresponding ABTS measurements (see Fig. 3C). In striking contrast, in the absence of Y10 (rodent $\text{A}\beta$, Y10-single and -double mutants) no dityrosine formation was observed at all, proving the specificity of the fluorescence measurements.

The formation of dityrosine bridges in $\text{A}\beta_{1-16}$ due to the peroxidase activity of $\text{A}\beta$ -heme complexes was reconfirmed using MALDI-TOF mass spectrometry (Supplementary Figure 3). As illustrated by the representative spectra shown in Supplementary Figure 5A-C, in the absence of H_2O_2 (dashed lines) only peaks at m/z 1956.0 ($\text{A}\beta + \text{H}^+$) followed by a typical isotopic pattern were found, corresponding to monomeric $\text{A}\beta_{1-16}$. In the absence of any further additions (Supplementary Figure 3A), the incubation of the peptide with 100 μM H_2O_2 (straight line) did not lead to any new peaks. The same holds for the addition of H_2O_2 to 100 μM peptide in the pres-

ence of 1 μM heme (Supplementary Figure 3B). In contrast, upon incubation of A β with H $_2$ O $_2$ in the presence of 2 μM heme (Supplementary Figure 3C), a new peak at m/z 3911.2 (A β -A β + H $^+$) was found, corresponding to dimeric A β_{1-16} with a dityrosine bridge. Again this new peak was followed by a typical isotopic pattern. A much more prominent dityrosine formation was observed after incubation of A β_{1-16} with H $_2$ O $_2$ and 1 μM HRP (Fig. 5D). An average relative dityrosine formation of $39.6 \pm 9.0\%$ was observed in the HRP-containing sample while in the presence of 2 μM heme only about $3.1 \pm 0.7\%$ was found, indicating a weak but still notable peroxidase activity in the latter case. Although not visible in the given sample (Supplementary Figure 3D), the statistical analysis showed that in the presence of HRP even in the absence of H $_2$ O $_2$ (dashed line) a small dityrosine formation ($2.6 \pm 1.4\%$) takes place.

Effect of peroxidase activity of A β -heme complexes on A β fibrillation

The ThT-based fluorescence measurements suggest inhibitory effects of free heme and H $_2$ O $_2$ on the fibrillation of A β_{1-40} . Moreover, upon co-incubation of higher amounts of HRP or higher heme concentrations with H $_2$ O $_2$, a totally different kinetics of the fluorescence increase was observed, possibly implicating a peroxidase-mediated change in the A β fibrillation behavior. However, as verified by STEM in all samples, a formation of A β fibrils took place while differences in the morphology were clearly observable.

As shown in Fig. 5A in the absence of further additions the incubation of A β_{1-40} (50 μM , black dashed line) with ThT led to a typical sigmoidal increase in the fluorescence with a fibrillation half-time ($t_{1/2}$) of 51.60 ± 0.01 h and an apparent rate constant (k_{obs}) of

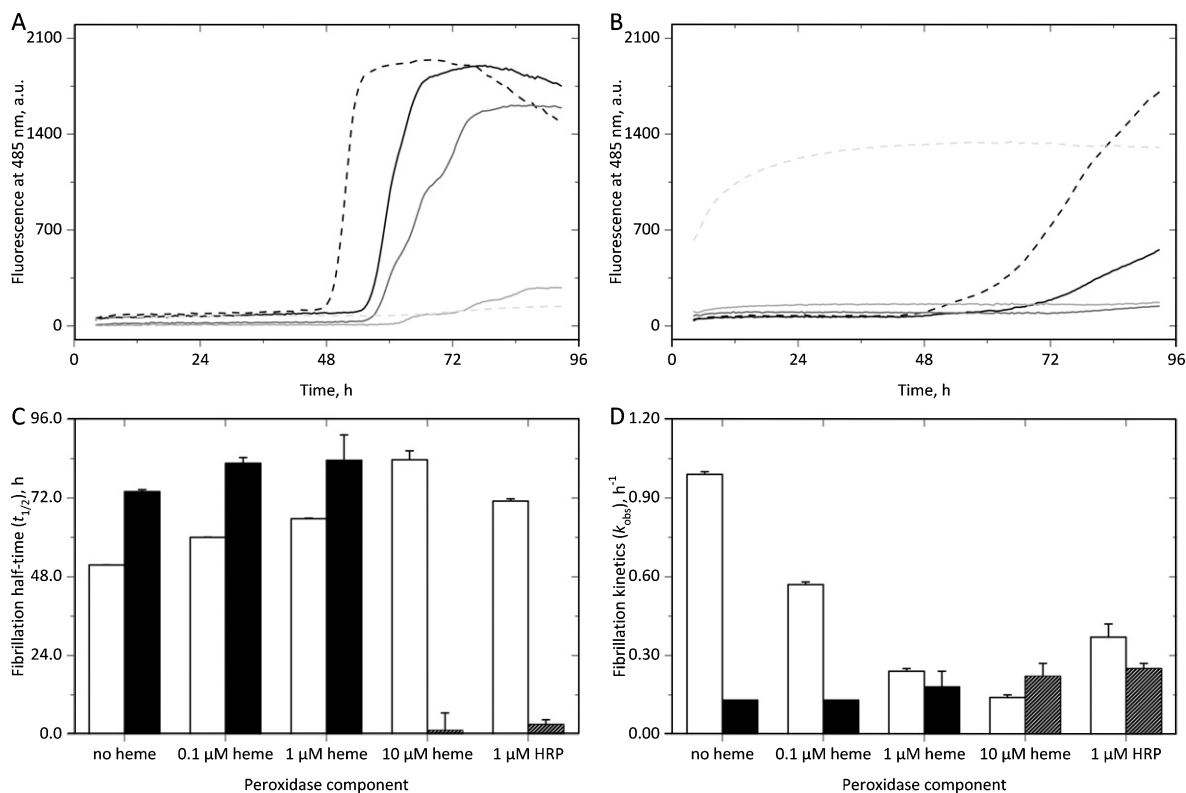


Fig. 5. Effect of heme-derived peroxidase activity on the A β fibrillation kinetics. A β_{1-40} (50 μM) was pre-incubated with free heme (0.1–10 μM , dark – light grey) or HRP (1 μM , light grey, dashed) in the absence (A) or presence (B) of H $_2$ O $_2$ (500 μM) before adding ThT (20 μM). Without H $_2$ O $_2$ (A) for the peptide alone (black, dashed), a $t_{1/2}$ value of 49.58 ± 0.99 h and a k_{obs} value of 0.99 ± 0.01 h^{-1} was observed while increasing heme concentrations constantly delayed and decreased the ThT-dependent fluorescence. In the presence of 1 μM HRP, almost no fluorescence intensity increase was observed. Also H $_2$ O $_2$ alone (B) inhibited the fluorescence increase while the additional presence of free heme increased the effect. In the presence of H $_2$ O $_2$ and 10 μM heme or 1 μM HRP, a slight (heme) or strong (HRP) hyperbolic increase in the ThT-derived fluorescence was observed instead of a sigmoidal kinetics. In (C) and (D), the $t_{1/2}$ and k_{obs} values are given for the experiments without (white) or with (black) H $_2$ O $_2$ whereby sometimes a logistic curve fit (dashed) was applied.

$0.99 \pm 0.01 \text{ h}^{-1}$ (see also Supplementary Table 1). Yet the curves observed after incubation with free heme (0.1–10 μM , dark grey – light grey lines) show a continuous shift in the lag phase as well as lower final fluorescence values, indicating a delay and partial inhibition of the A β fibrillation. In fact, in the presence of 10 μM heme, $t_{1/2}$ and k_{obs} values of $83.65 \pm 2.71 \text{ h}$ and $0.14 \pm 0.01 \text{ h}^{-1}$ were observed, suggesting a delayed and impaired formation of A β fibrils. Most interestingly in the presence of HRP (1 μM , light grey dashed line), almost no increase in the ThT-derived fluorescence was observed within 96 h, which may indicate an efficient inhibition of the A β fibrillation in the presence of the peroxidase. A fibrillation half-time of $71.07 \pm 0.66 \text{ h}$ and a k_{obs} value of $0.37 \pm 0.05 \text{ h}^{-1}$ were determined under these conditions.

As shown by the kinetic curves in Fig. 5B, after pre-incubation of A β_{1-40} with 500 μM H $_2\text{O}_2$ (50 μM , black dashed line) the ThT-based fluorescence measurements showed a delayed ($t_{1/2}$: $73.96 \pm 0.59 \text{ h}$) and slower (k_{obs} : $0.13 \pm 0.00 \text{ h}^{-1}$) increase in the fluorescence, indicating again a disturbed fibrillation of the peptide. Upon co-incubation of A β with 500 μM H $_2\text{O}_2$ and free heme (0.1–10 μM , dark grey – light grey lines), a further delay and decrease in the fluorescence intensity increase was observed. Of note, at 10 μM heme a fitting of the kinetic data to a sigmoidal curve was no longer possible. Instead a hyperbolic equation was applied, which better meets the small initial fluorescence increase observed under the described conditions. As shown in Supplementary Table 1, in this sample the half-maximal fluorescence intensity was achieved after about $1.15 \pm 5.33 \text{ h}$. Most interestingly also in the presence of 500 μM H $_2\text{O}_2$ and HRP (1 μM , light grey dashed line) an instant fluorescence increase was observed. The curve fitting revealed a $t_{1/2}$ value of $2.97 \pm 1.42 \text{ h}$. Both half-times lay within the 4 h ThT-free pre-incubation time of A β_{1-40} with heme, HRP, and/or H $_2\text{O}_2$.

In Fig. 5C, the $t_{1/2}$ values of all samples are compared whereby the white bars represent the H $_2\text{O}_2$ -free samples while in black the results obtained in the presence of H $_2\text{O}_2$ are given. This representation clearly shows the retarding effect of free heme, HRP, and H $_2\text{O}_2$ on the A β_{1-40} fibrillation as illustrated by higher fibrillation half-times of the ThT-sigmoidal fluorescence increase. In striking contrast, upon incubation of the peptide with 500 μM H $_2\text{O}_2$ and either 10 μM heme or 1 μM HRP a hyperbolic fluorescence

increase and considerably lower $t_{1/2}$ values were observed (dashed), suggesting different fibrillation kinetics of A β under these conditions. Maybe the peroxidase activity of HRP/A β -heme complexes is responsible for these differences. In Fig. 5D, the corresponding k_{obs} values are shown, clearly illustrating the decelerating effect of free heme on the ThT-derived fluorescence increase even in the absence of H $_2\text{O}_2$. In the presence of H $_2\text{O}_2$, even slower values were observed, which, however, increased slightly at higher heme concentrations. In the presence of 500 μM , H $_2\text{O}_2$ and either 10 μM heme or 1 μM HRP a comparable k_{obs} value was obtained from the applied logistic curve fitting (dashed).

We also created STEM pictures of the described samples to confirm the A β fibrillation as well as to study the long-term effect of free heme, HRP, and H $_2\text{O}_2$ on the formation of peptide fibrils. As illustrated by the representative microscopic pictures given in Fig. 6, both in the absence (Fig. 6A-E) and in the presence (Fig. 6F-J) of H $_2\text{O}_2$, an ultimate formation of A β fibrils was observed. Thereby an average fibril diameter of $14.4 \pm 2.3 \text{ nm}$ was observed throughout the samples. However, differences in the fibril morphology and density were sometimes clearly visible. While the presence of 0.1 μM heme (Fig. 6B, G) and/or 500 μM H $_2\text{O}_2$ (Fig. 6F, G) seem to have no effect on the fibrillation of 50 μM A β_{1-40} (A) in the presence of 1 μM (Fig. 6C, H) or 10 μM (Fig. 6D, I) heme, the formation of a more dense A β fibril network seems to take place. Thereby, more amorphous fibrils were observable in the absence of H $_2\text{O}_2$ (Fig. 6C, D), while in the presence of H $_2\text{O}_2$ (Fig. 6H-I), straight and dense fibrils were visible. In the presence of HRP (Fig. 6E, J), again amorphous fibrils were observed in the absence of H $_2\text{O}_2$ (Fig. 6E), while in the presence of H $_2\text{O}_2$ (Fig. 6J), straight and dense fibrils were visible. Yet in the latter case, much less fibril formation was observed as compared to the heme-containing samples.

Determination of A β -derived cerebral angiopathies in vivo

The MRA measurements clearly showed a decreased blood flow in the middle cerebral artery (MCA) in the Tg2576 mice, correlating well with the increased perivascular deposition of A β in this AD model. Moreover, a co-localization of the peptide with free iron was observed in the brain tissue of the animals.

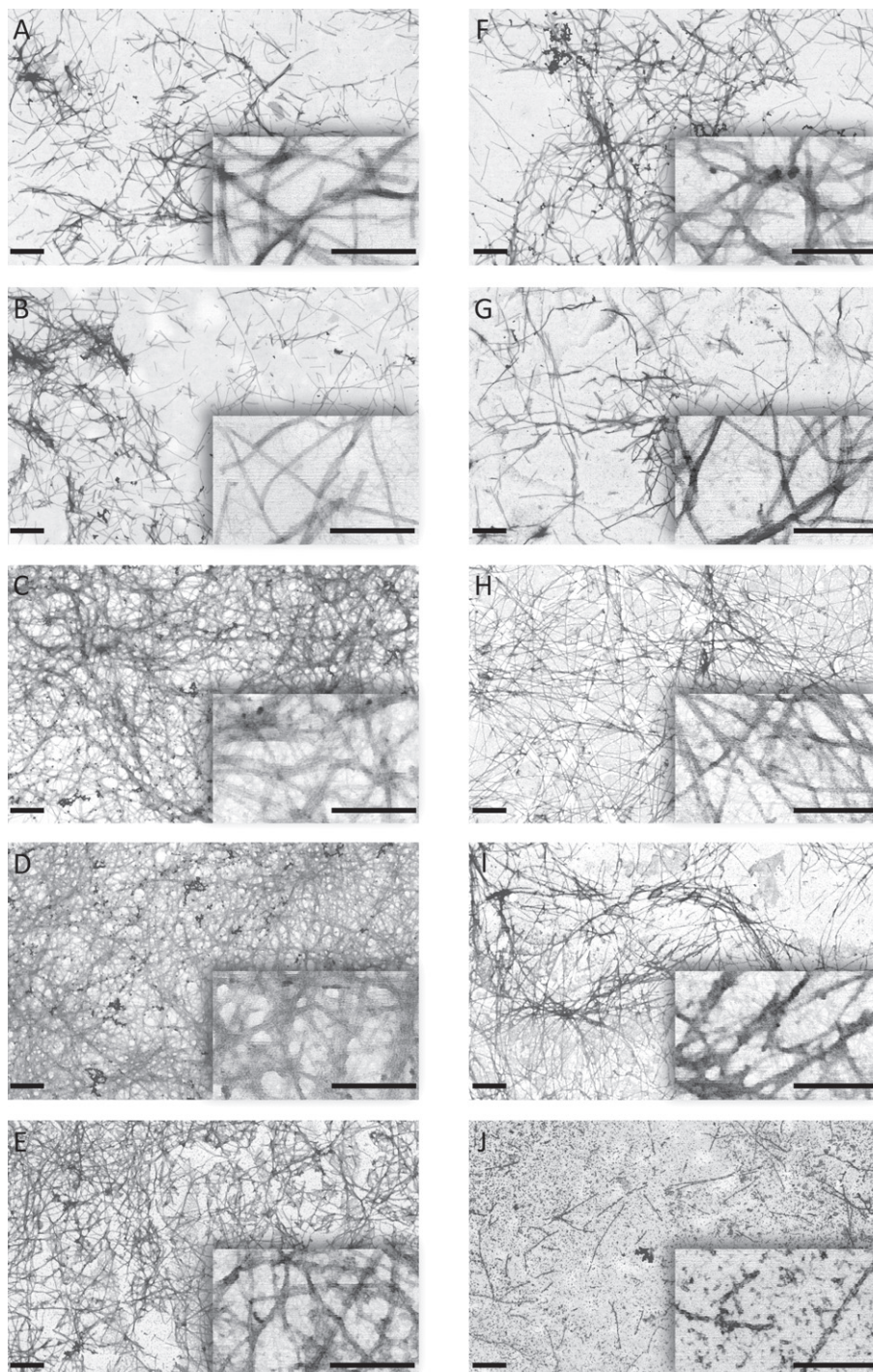


Fig. 6. A β fibril formation in the presence of peroxidase components. A β ₁₋₄₀ (50 μ M) was pre-incubated with 0 μ M (A, F) – 10 μ M heme (D, I) or 1 μ M HRP (E, J) either in the absence (A-E) or presence (F-J) of 500 μ M H₂O₂. After 4 h, ThT (20 μ M) was added for the kinetic measurements given in Fig. 5. The shown representative STEM pictures were taken from samples prepared about 10 days after the ThT measurements. In all samples, A β fibrils with an average diameter of 14.4 ± 2.3 nm are clearly visible (see inserts) while differences in the overall fibril structure morphology and density (see overview) were observed. Especially in the presence of higher heme concentrations, a denser but more amorphous fibril network was observed in the absence of H₂O₂ (C-D) while in the presence of H₂O₂, the fibril network resembled the negative control (A, neither heme nor H₂O₂). In the sample containing HRP and H₂O₂ (J), a less and shorter fibrils were observed. The scaling bars correspond to 500 nm (overview) and 250 nm (inserts).

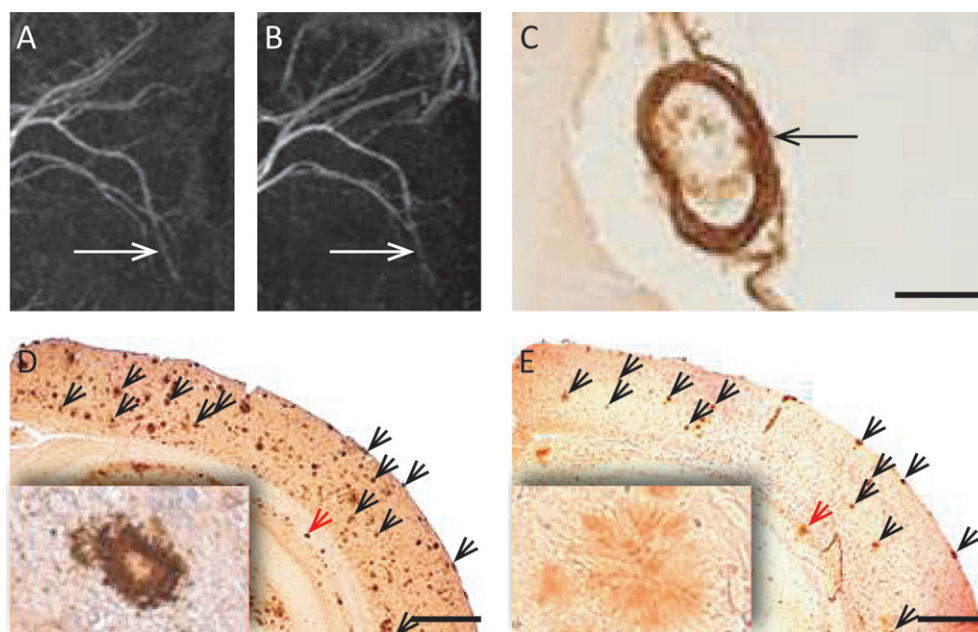


Fig. 7. Blood flow disturbances and co-localization of A β and iron in Tg2576 mice. MRA measurements were performed for the visualization of the blood vessels while CAA, A β deposits, and iron accumulation were detected via staining of the brain sections. While the angiogram of an 18-month-old healthy control animal (A) showed no blood flow alterations, in the corresponding picture of a Tg2576 mouse (B) blood flow defects are clearly visible (arrow). As shown in (C), the latter correspond with a marked deposition of A β ₁₋₄₀ (arrow) in the pial branches of the MCA. Moreover, in the Tg2576 mice a co-localization of A β plaques (D) and iron (E) in the adjacent brain sections was observed (small arrows). The inserts given in (D-E) represent an about 8-fold magnification of the regions marked with the red arrows. The scaling bars correspond to 500 μ m (C) and 50 μ m (D-E).

As A β is responsible both for microhemorrhages [53] and for erythrocyte alterations [54] in AD, we finally performed *in vivo* measurements to illustrate a possible pathway for the formation of A β -heme complexes at AD. As illustrated in Fig. 7A-B, the MRA studies showed a marked disturbance of the blood flow in the branches of the MCA of Tg2576 mice (Fig. 7B), while in the healthy control (Fig. 7A) normal signal intensities were observed throughout the vessels. In both cases, a sagittal view of the head of age-matched (18 months) animals is shown. The identification of cerebral arteries was performed by inspecting the angiograms under various angles and comparing the vessels to literature data [49, 55–57].

As illustrated by the microscopic picture given in Fig. 7C, the blood flow disturbances in the AD model animals coincide with the massive deposition of A β ₁₋₄₀ in the territory of the pial branches of the MCA. In the healthy control animals, no accumulation of the peptide in the vessel walls was observable (not shown). Furthermore, the analysis of adjacent brain sections showed a coincidence of amyloid plaques (Fig. 7D) with the deposition of free iron (Fig. 7E) in the Tg2576 mice. These results

leave open the possibility that the iron could be the leftover of free heme, which, considering the CAA shown in Fig. 7A-C, may result from microhemorrhages and hemolytic events in the brain tissue of AD patients. In summary, the detected A β -derived blood flow alterations and the co-localization of free iron with A β plaques may indicate the transient formation of A β -heme complexes during the pathology of AD.

DISCUSSION

The applied system is suitable to test the peroxidase activity of A β -heme complexes

In this study, ABTS-based absorbance measurements were used as a well-established method to study the peroxidase activity of A β -heme complexes [19]. Thereby we followed the ABTS^{•+} formation at 734 nm to avoid interferences from other assay components [36] including free heme [58, 59]. Furthermore, most experiments were conducted at an excess of ABTS to avoid over-oxidation to ABTS²⁺

and related side products [60]. The small absorbance decrease observed at longer measuring times may be attributed to ABTS backformation [60]. It was mainly observed in the presence of tyrosine-containing A β sequences, suggesting a radical transfer to the peptide. The measurements with free heme in the absence of A β yielded activities of 0.13 mU/ml (1 μ M heme) and 1.03 mU/ml (10 μ M heme), respectively, proving an adequate correlation between the concentration of the peroxidase-active component and the determined initial enzymatic activity.

A β promotes the peroxidase activity of free heme in a concentration-dependent way

The ABTS measurements clearly showed that A β promotes the peroxidase activity of free heme in a concentration-dependent manner. Thereby at ratios higher than 20:1 a saturating effect was observed, maybe indicating the formation of A β -heme complex with the named stoichiometry. Comparable results were also observed in other studies whereby, however, only ratios up to 8:1 were applied [19, 27, 61]. In line with others in the absence of free heme, we observed no peroxidase activity [25], proving a heme-based enzymatic activity of A β -heme complexes.

The relative effect of A β on the heme-derived peroxidase activity also depended on the absolute heme concentration: At higher heme concentrations, stronger effects of the peptide were observed. These results indicate the formation of A β -heme complexes with multiple heme units. Moreover, they suggest a non-linear increase in the peroxidase activity upon cerebral accumulation of free heme, especially in the presence of elevated A β levels observed in AD patients.

Another new aspect addressed in this study is the H₂O₂ dependence of the A β -heme complex-mediated peroxidase activity. Thereby either H₂O₂ was directly applied or the G/GO-system was used, which allows a continuous H₂O₂ production [62]. A direct comparison of the H₂O₂ concentration-dependent increase in the relative peroxidase activity yielded comparable effects for free heme (10 μ M) and for A β -heme complexes (10 μ M/1 μ M), again proving a heme-based peroxidase activity of the complexes. Still at higher constant H₂O₂ production rates, a stronger promotion of the enzymatic activity with increasing A β concentrations was observed, which may indicate a coordinating effect of the peptide with regard to the heme activation by H₂O₂.

In fact, in chordata heme peroxidases, the amino acids on the distal heme site are known to regulate the access of H₂O₂ toward the heme center [63, 64].

Selected studies at pH 6.5 showed higher peroxidase activities of A β -heme complexes as compared to the values obtained at pH 7.4. While the pH-dependent peroxidase activity of A β -heme complexes was never tested before, these results are well in line with the results obtained with heme peroxidases [63, 64]. The studies also revealed an influence of the pH value on the A β -derived promotion of the peroxidase activity, showing a stronger effect of the peptide at neutral conditions. These results can be explained by the fact that both, the binding of the peptide to heme [27] and the subsequent promotion of the heme-mediated peroxidase activity are influenced by the pH value [25, 35]: While for the binding of the heme a histidine residue (most likely H13) with a neutral net charge is responsible [19, 33, 65], an acidic arginine (R5) promotes the stabilization of H₂O₂ as the sixth heme ligand [20] and its subsequent homolytic cleavage [15, 19, 27]. Y10 is regarded as the second amino acid contributing to the peroxidase activity of A β -heme complexes [15, 25].

As up to low micromolar heme concentration were found in the brain tissue of AD patients, the performed peroxidase activity measurements (1/10 μ M heme) are somewhat comparable to the physiological conditions [28]. Yet the applied A β concentrations (up to 100 μ M) are far beyond the physiological range [66, 67]. Still such high peptide concentrations were necessary to explore the A β -heme ratio-dependent peroxidase activity. Moreover, the aggregation of A β as well as its deposition around blood microvessels [53, 68] may lead to high local concentrations of the peptide, especially at places of hemolysis-derived formation of free heme. Regarding H₂O₂ again unphysiological high concentrations were applied. Still the lowest concentration used in our studies (20 μ M, see Fig. 2B) approximately meet (patho-) physiological H₂O₂ concentrations in the blood [69]. In contrast, by using 500 μ M H₂O₂, a suitable high peroxidase activity could be observed to investigate, e.g., the A β sequence-dependent enzymatic activity of A β -heme complexes.

The three amino acids responsible for the binding (H13) of free heme and the subsequent peroxidase activity of A β -heme complexes in the presence of H₂O₂ (R5, Y10) resemble the corresponding structures in chordata heme peroxidases [19, 27, 70]. Moreover, they represent the only differences between

the human and the mouse sequence of the peptide [19, 20]. While we included only peroxidase activity experiments with A β ₁₋₁₆ in the manuscript some preliminary experiments as well as literature data [61] clearly indicate a much higher peroxidase activity of the long peptide in the presence of free heme.

Human A β has the strongest impact on the peroxidase activity of free heme

We next tested the impact of the peptide sequence of A β ₁₋₁₆ on the promotion of the heme-mediated peroxidase activity. Thereby special attention was paid to the three amino acids mutated in the human peptide (R5, Y10, H13) in comparison to the rodent peptide (G5, F10, R13). Already published mutational studies only cover a direct comparison between human A β and the rodent equivalent [27] or the replacement of single human-specific A β amino acids by non-rodent equivalents, namely R5N, Y10G, and H13A [19, 25]. Still the reported results are comparable to ours: While others also clearly showed a lower peroxidase of A β -heme complexes formed with the rodent peptide as compared to complexes formed with human A β , the differences were not quantified and only A β -heme ratios up to 8:1 were used [27]. In our studies, the rodent peptide only doubled the peroxidase activity of free heme, while in the presence of the human peptide, an about 8-fold higher peroxidase activity was observed.

Regarding single mutants for Y10G a marked decrease in the peroxidase activity was reported [25], which corresponds to our results. In fact, in our studies Y10G turned out as the single mutant with the strongest effect, suggesting Y10 as an important key player during the peroxidase activity of A β -heme complexes. However, for the corresponding rodent mutation (Y10F), only an about 1.4-fold decreased peroxidase activity was observed. As suggested by a recent publication, the named mutants influence the structure of the peptide, which also affects the peroxidase activity of the formed A β -heme complexes [61]. Regarding the artificial mutation R5N, again a strong decreasing effect on the peroxidase activity was reported [19], which is only partially reflected by our results. Again, the corresponding rodent single mutation (R5G) had a weaker effect. These differences may be attributed to varying experimental conditions, including the applied A β -heme ratio and H₂O₂ concentration. Another possible explanation comes from a recently published review: As stated by Kohdarahmi et al., R5 may have only a minor effect on the perox-

idase activity of A β -heme complexes, most likely by influencing the structure and/or aggregation behavior of A β [61].

For H13A (and H14A), almost no effect on the peroxidase activity was reported, which was attributed to the fact that H13 (present in human A β) can be replaced by H14 (present in human and rodent A β), and *vice versa*, in regard to the binding of free heme [19]. Accordingly for the H13G, H14G double mutation, a peroxidase activity at the level of free heme was observed [19]. Regarding the single mutants, the results are only partially comparable to ours where a single mutation of H13 (H13R or H13A) already led to a considerably decreased peroxidase activity. Yet in line with others [19], upon application of the H13G, H14G double mutation, we observed a massive reduction of the peroxidase activity. In fact, the obtained value was even slightly lower than the peroxidase activity obtained in the presence of free heme and rodent A β ₁₋₁₆. Yet unlike shown by others, it still exceeded the peroxidase activity observed in the sole presence of free heme [19].

As reported previously [61], for human A β (see Fig. 1), but not, for example, for the murine peptide, increasing A β -heme ratios lead to a considerable increase in the peroxidase activity. Thus, the differences obtained by using a 10/1 ratio may be small by applying equimolar A β -heme complexes.

In summary, regarding the tested single mutants, the replacement of Y10 showed the strongest effect, while lower impacts were found for H13 und R5. Yet considering that H13 may be replaced by H14 [33], the strongest impact was found for histidine (H13/H14), followed by the human-specific residues Y10 and R5. In fact, H13/14 is responsible for the binding of free heme [26, 27, 65] while Y10 and R5 contribute to the subsequent peroxidase activity of A β -heme complexes [19, 25]. Most interestingly Y10 is not only regarded as a redox-active center contributing to the peroxidase activity of A β -heme complexes [19] but also as an endogenous target for this enzymatic activity, leading to the formation dityrosine [21, 25, 29].

Human-specific Y10 is an endogenous peroxidase substrate of A β -heme complexes

Our studies confirmed the results of others [21, 25] that upon peroxidase activity of A β -heme complexes Y10 can be oxidized to form 1,3-dityrosine [42, 71]. Yet the impact of the A β -heme ratio and the amount of H₂O₂ on the dityrosine yield was never tested before.

Our fluorescence measurements suggest an optimal dityrosine formation at an A β -heme ratio of about 40:1, which contradicts the continuous increase of the peroxidase activity at higher peptide excesses. These apparently discrepant results may be explained by the fact that a strong peroxidase activity leads to the over-oxidation of tyrosine to products like trityrosine, isotrityrosine, and pulcherosine, which decrease the amount of dityrosine [71, 72]. Both upon direct addition of H₂O₂ and by applying the G/GO-system a greater dityrosine yield was obtained at higher H₂O₂ concentrations, which suggests that multiple peroxidase cycles of the A β -heme complexes are needed per dityrosine molecule to be formed.

Another new aspect addressed in this work is the effect of the A β ₁₋₁₆ sequence on the dityrosine formation. In line with others, in the absence Y10 we observed no dityrosine formation at all, proving the specificity of the fluorescence measurements [19, 25]. Yet by testing single and double mutants of human A β ₁₋₁₆, we also observed an influence of R5, H13, and H14 on the dityrosine yield: Strangely enough, by replacing the named amino acids by the rodent or an artificial equivalent, we always observed an at least slightly higher dityrosine formation. The most striking differences were observed for the H13R single mutant and the H13G, H14G double mutant were a doubled (H13R) and a not significantly reduced (H13G, H14G) dityrosine yield coincide with a slightly (H13R) or strongly (H13G, H14G) reduced peroxidase activity. As the named histidine residues are responsible for the proximal heme coordination, we guess that their replacement leads to the formation of less stable A β -heme complexes [19]. Accordingly, a lower peroxidase activity is observed, which, however, may translate to a higher dityrosine yield as over-oxidations and/or the formation of other tyrosine oxidation products than dityrosine are diminished [71, 72].

To confirm the formation of dityrosine upon A β -heme peroxidase activity, we also performed selected MALDI-TOF measurements. While in the presence of H₂O₂ we were able to show a minor dityrosine formation in the presence of free heme and a moderate product formation in the presence of HRP, the obtained product yields are scarcely comparable to the fluorescence measurements. Given the limited quantification of mass spectrometry data, in future studies dityrosine antibodies [19, 21, 25] or thin-layer chromatography [71] should be applied. As a mechanism for the reported dityrosine formation,

we propose a direct one-electronic oxidation by the activated A β -heme peroxidase [73], followed by a recombination of the formed tyrosyl radicals. In fact, Y10 is located directly at the active site of in A β -heme complexes, suggesting a direct oxidation by the activated oxoferryl state [28]. Yet it has to be stated that free ROS, including hydroxyl radicals (\cdot OH) [74], may also lead to A β -derived dityrosine formation under oxidative stress conditions of AD [42].

In summary, the obtained results clearly show the formation of dityrosine from Y10 due to the peroxidase activity of A β -heme complexes. As already reported in the literature the Y10-derived dityrosine formation in the presence of H₂O₂ [25] promotes the aggregation of A β via stabilization of peptide dimers [21, 28, 29], which may be relevant for the progression of AD.

The formation of A β -heme complexes has several effects on A β fibril formation

Yet while A β -heme complex-mediated dityrosine formation promotes the fibrillation of the peptide, free heme is well known to inhibit A β aggregation [33] and even leads to the dismantling of partly formed fibrils [26, 31]. In fact, free heme interacts both with H13/H14, leading to the formation of peroxidase-active A β -heme complexes [27], and with F19/F20, which inhibits the fibrillation of the peptide [3, 26, 33]. Yet the mentioned studies on A β fibrillation in the presence of free heme have often been performed only at low A β -heme ratios [26, 31], lack long-term observation [31] and do not include the application of H₂O₂ [75] as a precondition for the A β -heme complex-derived dityrosine formation. By using ThT-based fluorescence measurements [31], in this study the named issues were addressed and clearly showed that even at low ratios (50:0.1) free heme already starts to delay and inhibit the formation of A β fibrils. Still it has to be stated that the initial interaction of ThT with the negatively charged peptide is of electrostatic nature [44, 45], which may provide an additional explanation for the observed lower fluorescence values.

Most interestingly also H₂O₂ itself apparently disturbed the formation of peptide fibrils. Yet these results may also be explained by the fact that oxidized A β fibrils yield a weaker fluorescence signal than native ones during the ThT measurements [21]. Moreover, we cannot rule out a direct oxidation of the dye. The same holds for the measurements in the presence of H₂O₂ and heme or HRP as well as for the

HRP control. One interesting aspect observed during the measurements with ThT is the different kinetics in the fluorescence increase observed after application of 1 μ M HRP or 10 μ M heme and H₂O₂: In both cases a hyperbolic instead of sigmoidal fluorescence increase was observed. To our knowledge, such results were never obtained before and may indicate a completely different fibrillation behavior of A β in the presence of peroxidase activity [47].

The also performed STEM measurements clearly showed that despite the (apparent) inhibitory effect of heme, H₂O₂, and HRP on the A β fibrillation within the first 96 h, in all samples a peptide fibrillation finally takes place. Thereby A β fibrils with a diameter of about 14 nm were always observed, which is in the expected range [21, 34]. Still, while in the sole or combined presence of H₂O₂ or low amounts of free heme, the fibrils strongly resembled the control (A β ₁₋₄₀ alone) at higher heme concentrations or in the presence of HRP different fibril morphologies were found. These results are in line with others [21] who also observed different fibril networks under oxidative conditions [21]. The observed denser fibril

networks in the sole presence of higher heme concentrations are somewhat surprising as no peroxidase activity should take place in the absence of H₂O₂. Yet it may be explained by the release of free iron, which is well known to promote the aggregation of A β [26].

In summary, ThT measurements, especially at the chosen experimental conditions [44, 45], are a suitable tool to show the strong inhibitory effect of free heme on A β fibrillation. Yet they are not completely reliable under conditions where oxidative processes take place. Still the STEM measurements clearly indicate that the A β -heme complex-derived peroxidase activity influences the fibril morphology. Most likely the formation of dityrosine disturbs the classical A β fibrillation pathway, leading to an enhanced formation of, e.g., protofibrils [34]. This is nicely illustrated by the positive control (HRP + H₂O₂) where thinner and shorter fibrils were observed. Thus, free heme, upon complexation with A β , subsequent peroxidase activity and dityrosine formation, actually seems to promote the dimerization/oligomerization of the peptide.

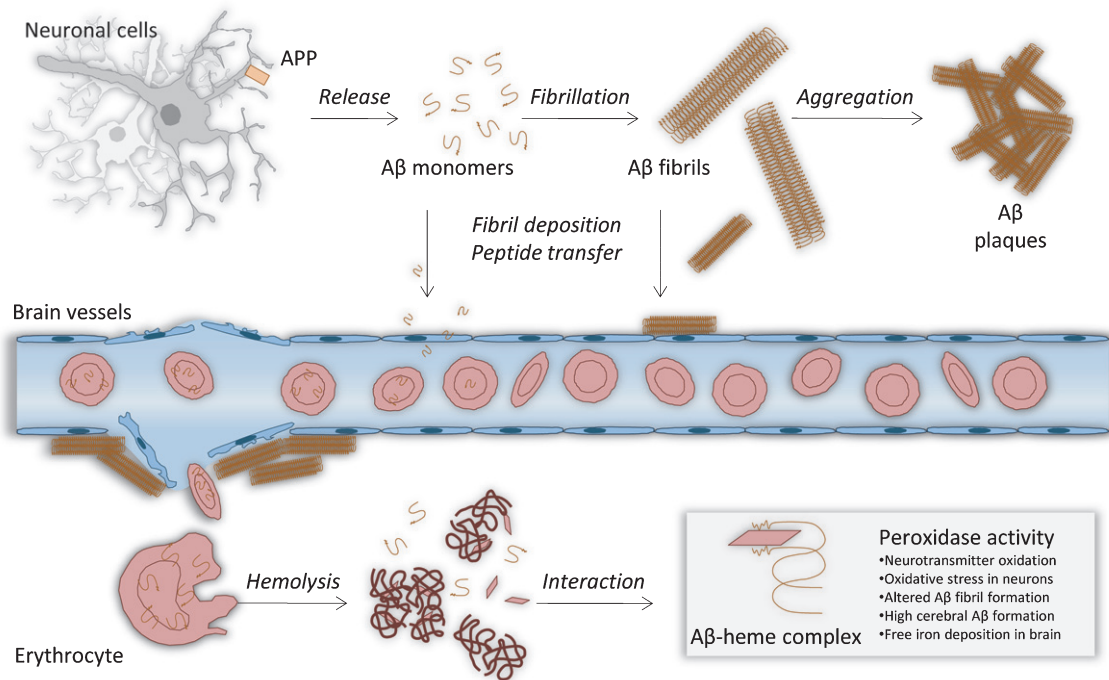


Fig. 8. Proposed model for A β -derived microvessel destruction and hemolysis as a source for cerebral free heme. While monomeric A β readily crosses the blood-brain barrier, A β fibrils deposit around cerebral blood vessels and lead to microhemorrhages. A subsequent A β monomer and/or fibril-derived hemolysis of erythrocytes leads to the accumulation of free heme in the brain tissue. Especially in the presence of elevated cerebral A β levels, these processes will lead to the formation of A β -heme complexes, which, in the presence of H₂O₂, exhibit a peroxidase activity. The latter causes, e.g., oxidative stress in the brain tissue, neuronal death, and neurotransmitter destruction, thus, may considerably contribute to the pathology of AD.

While Alzheimer plaques contain both A β ₁₋₄₀ and A β ₁₋₄₂, in the current study, the shorter peptide was used as it was already discussed as the more toxic one, maybe due to its slower aggregation as compared to A β ₁₋₄₂ [16]. Moreover besides this small difference in the aggregation kinetics both peptides were reported to be well comparable regarding their affinity toward heme [33]. Thus, our results are most likely well transferable to A β ₁₋₄₂.

Yet it has to be clearly stated that the peroxidase activity measurements performed with A β ₁₋₁₆ are only partly comparable to the aggregation studies performed with the full length peptide: As discussed in a recent publication [61], free heme most likely binds not only to H13/H14 in the hydrophilic part of the peptide but also to F19/20 in the hydrophobic part of A β _{1-40/42} [26, 27]. In fact, the latter second heme binding site was already shown to affect the peroxidase activity of A β -heme complexes [37].

Most interestingly as even in mature A β fibrils the amino acids responsible for the formation of peroxidase-active A β -heme complexes (R5, Y10, H13/H14) are part of the unstructured solvent-facing side chains [11, 76, 77]. Accordingly, the aggregation state of the peptide was shown to have no influence on this enzymatic activity [3, 37]. In fact, a recent review shows a positive correlation between A β aggregation and the peroxidase activity of A β -heme complexes [61]. In line with our results, this effect is attributed to peroxidase complexes with an A β -heme ratio higher than one [28, 61]. The last question addressed in this study refers to possible sources of free heme as a precondition for the formation of A β -heme complexes in the brain tissue of AD patients.

A β -derived CAA and hemolysis could lead to the formation of A β -heme complexes

We also performed MRA measurements and, as reported before [49], detected a decreased blood flow in Tg2576 mice as compared to the healthy control. Thereby in line with others [53, 66], a clear correlation with the vascular deposition of A β was observed. Furthermore, in the animals a co-localization of free iron with A β plaques was found, which again confirms published results [20, 21].

Originally a disturbed mitochondrial heme metabolism in neurons was suggested as a source for free heme and iron in the brain [23, 78]. Yet, based on the obtained results and literature studies,

we suggest that hemoglobin may represent the major for cerebral free heme in AD. As illustrated in Fig. 8, the vascular deposition of A β (CAA) [6], resulting cerebral microhemorrhages [53, 68] and the hemolytic effect of the peptide [54, 66] could account as the major mechanisms. This theory is confirmed by the fact that hemolysis-associated acute phase proteins like Hpx [4, 79] and heme oxygenase 1 [80, 81] show a higher expression in AD patients. Moreover, hemoglobin-derived peptides are elevated in the brain of AD patients [82].

In blood, A β is quickly taken up by erythrocytes and leads to increased cell sizes and decreased deformability of the cells [66, 67]. This effect, which leads to hemolytic events in the tight brain capillaries [83], was already attributed to the induction of oxidative stress in the erythrocytes [54, 84]. Thus, we cannot rule out a contribution of A β -heme complex-mediated peroxidase activity during these processes. Most interestingly, A β was also shown to inactivate catalase in erythrocytes, leading to an increased H₂O₂ concentration in these cells [85]. Moreover, A β -derived phospholipid oxidation in erythrocytes leads to increased endothelial binding of the cells [86, 87] and vascular destructions [86], providing positive feedback mechanisms for the accumulation of erythrocytes and free heme in the brain tissue. Up to micromolar cerebral heme concentrations were found in AD patients [28]. In addition endothelial and smooth muscle cells of cerebral microvessels can also produce A β PP [53], a process, which may be elevated upon A β -derived microhemorrhages.

Thus, the presented *in vivo* results confirm already published pathological features of AD, including CAA as well as the coinciding deposition of A β plaques and free iron. Still, considering literature data these observations may represent final remains of A β -derived microhemorrhagic and hemolytic events, which could lead to the formation of blood-derived A β -heme complexes as a possible hallmark of AD pathology. Accordingly, AD was already suggested as a thrombohemorrhagic disorder [88] whereby A β -heme complexes play a key role [20]. In fact, these complexes are most likely also formed *in vivo* and the resulting peroxidase activity contributes to the pathology of AD [89]. In order to prove the connection between CAA, in future studies we will try to detect free heme in the brain tissue of Tg2576 mice [28]. Furthermore dityrosine formation in the brain tissue of this AD model will also be addressed [90]. In sum-

mary, realizing the peroxidase activity of A β -heme complexes as an important pathological mechanism of this neurodegenerative disease may open the door for the development of new therapeutic strategies, including the application of antioxidants [22, 24] and/or heme peroxidase inhibitors [34]. Recently also the binding of free heme to the tau protein was shown [91], suggesting an even broader role of free heme at AD. Hyperphosphorylated tau protein and tau-containing neurofibrillary tangles are major hallmarks of AD besides A β plaques [20, 92].

ACKNOWLEDGMENTS

We thank Uladzimir Barayeu for his help to set up the G/GO-system. The study was supported by the DFG (SFB-TRR 102, A06). We also thank the Alzheimer Forschung Initiative e.V. for the financial support (AFI, Grant Nr. 13810).

Authors' disclosures available online (<https://www.j-alz.com/manuscript-disclosures/17-0711r1>).

SUPPLEMENTARY MATERIAL

The supplementary material is available in the electronic version of this article: <http://dx.doi.org/10.3233/JAD-170711>.

REFERENCES

- [1] van Dam D, De Deyn PP (2011) Animal models in the drug discovery pipeline for Alzheimer's disease. *Br J Pharmacol* **164**, 1285-1300.
- [2] Cacciottolo M, Morgan TE, Finch CE (2016) Rust on the brain from microbleeds and its relevance to Alzheimer studies: Invited commentary on Cacciottolo Neurobiology of Aging, 2016. *J Alzheimers Dis Parkinsonism* **6**, 1-7.
- [3] Zhao LN, Mu Y, Chew LY (2013) Heme prevents amyloid beta peptide aggregation through hydrophobic interaction based on molecular dynamics simulation. *Phys Chem Chem Phys* **15**, 14098-14106.
- [4] Ringman JM, Schulman H, Becker C, Jones T, Bai Y, Immermann F, Cole G, Sokolow S, Gyls K, Geschwind DH, Cummings JL, Wan HI (2012) Proteomic changes in cerebrospinal fluid of presymptomatic and affected persons carrying familial Alzheimer disease mutations. *Arch Neurol* **69**, 96-104.
- [5] Martino Adami PV, Galeano P, Wallinger ML, Quijano C, Rabossi A, Pagano ES, Olivar N, Reyes TC, Cardinali D, Brusco LI, Do CS, Radi R, Gevorkian G, Castano EM, Cuello AC, Morelli L (2017) Worsening of memory deficit induced by energy-dense diet in a rat model of early-Alzheimer's disease is associated to neurotoxic Abeta species and independent of neuroinflammation. *Biochim Biophys Acta* **1863**, 731-743.
- [6] Mendel TA, Wierzb-Bobrowicz T, Lewandowska E, Stepień T, Szpak GM (2013) The development of cerebral amyloid angiopathy in cerebral vessels. A review with illustrations based upon own investigated post mortem cases. *Pol J Pathol* **64**, 260-267.
- [7] Chetelat G, Ossenkoppele R, Villemagne VL, Perrotin A, Landeau B, Mezenge F, Jagust WJ, Dore V, Miller BL, Egret S, Seeley WW, van der Flier WM, La JR, Ames D, van Berckel BN, Scheltens P, Barkhof F, Rowe CC, Masters CL, de La Sayette V, Bouwman F, RabinoVICI GD (2016) Atrophy, hypometabolism and clinical trajectories in patients with amyloid-negative Alzheimer's disease. *Brain* **139**, 2528-2539.
- [8] Kosenko EA, Aliev G, Kaminsky YG (2016) Relationship between chronic disturbance of 2,3-diphosphoglycerate metabolism in erythrocytes and Alzheimer disease. *CNS Neurol Disord Drug Targets* **15**, 113-123.
- [9] Jaremo P, Milovanovic M, Nilsson S, Buller C, Post C, Winblad B (2011) Alzheimer's disease is characterized by more low-density erythrocytes with increased volume and enhanced beta-amyloid x-40 content. *J Intern Med* **270**, 489-492.
- [10] Armstrong RA (2013) What causes Alzheimer's disease? *Folia Neuropathol* **51**, 169-188.
- [11] Riek R, Eisenberg DS (2016) The activities of amyloids from a structural perspective. *Nature* **539**, 227-235.
- [12] Walti MA, Ravotti F, Arai H, Glabe CG, Wall JS, Bockmann A, Guntert P, Meier BH, Riek R (2016) Atomic-resolution structure of a disease-relevant Abeta(1-42) amyloid fibril. *Proc Natl Acad Sci U S A* **113**, E4976-E4984.
- [13] Zheng H, Koo EH (2006) The amyloid precursor protein: Beyond amyloid. *Mol Neurodegener* **1**, 1-12.
- [14] Riek R (2017) The three-dimensional structures of amyloids. *Cold Spring Harb Perspect Biol* **9**, 1-12.
- [15] Bastianetto S, Menard C, Quirion R (2015) Neuroprotective action of resveratrol. *Biochim Biophys Acta* **1852**, 1195-1201.
- [16] Jiang T, Sun Q, Chen S (2016) Oxidative stress: A major pathogenesis and potential therapeutic target of antioxidative agents in Parkinson's disease and Alzheimer's disease. *Prog Neurobiol* **147**, 1-19.
- [17] Markesbery WR (1997) Oxidative stress hypothesis in Alzheimer's disease. *Free Radic Biol Med* **23**, 134-147.
- [18] Chen Z, Zhong C (2014) Oxidative stress in Alzheimer's disease. *Neurosci Bull* **30**, 271-281.
- [19] Lu N, Li J, Tian R, Peng YY (2014) Key roles of Arg(5), Tyr(10) and his residues in Abeta-heme peroxidase: Relevance to Alzheimer's disease. *Biochem Biophys Res Commun* **452**, 676-681.
- [20] Ghosh C, Seal M, Mukherjee S, Ghosh DS (2015) Alzheimer's disease: A heme-abeta Perspective. *Acc Chem Res* **48**, 2556-2564.
- [21] Al-Hilaly YK, Williams TL, Stewart-Parker M, Ford L, Skaria E, Cole M, Bucher WG, Morris KL, Sada AA, Thorpe JR, Serpell LC (2013) A central role for dityrosine crosslinking of amyloid-beta in Alzheimer's disease. *Acta Neuropathol Commun* **1**, 1-17.
- [22] Xie H, Hou S, Jiang J, Sekutowicz M, Kelly J, Bacskai BJ (2013) Rapid cell death is preceded by amyloid plaque-mediated oxidative stress. *Proc Natl Acad Sci U S A* **110**, 7904-7909.
- [23] Atamna H, Frey WH (2004) A role for heme in Alzheimer's disease: Heme binds amyloid beta and has altered metabolism. *Proc Natl Acad Sci U S A* **101**, 11153-11158.

- [24] Atamna H, Boyle K (2006) Amyloid-beta peptide binds with heme to form a peroxidase: Relationship to the cytopathologies of Alzheimer's disease. *Proc Natl Acad Sci U S A* **103**, 3381-3386.
- [25] Lu N, Li J, Tian R, Peng YY (2015) Key roles for tyrosine 10 in abeta-heme complexes and its relevance to oxidative stress. *Chem Res Toxicol* **28**, 365-372.
- [26] Yuan C, Gao Z (2013) Abeta interacts with both the iron center and the porphyrin ring of heme: Mechanism of heme's action on Abeta aggregation and disaggregation. *Chem Res Toxicol* **26**, 262-269.
- [27] Atamna H, Frey WH, Ko N (2009) Human and rodent amyloid-beta peptides differentially bind heme: Relevance to the human susceptibility to Alzheimer's disease. *Arch Biochem Biophys* **487**, 59-65.
- [28] Thiabaud G, Pizzocaro S, Garcia-Serres R, Latour JM, Monzani E, Casella L (2013) Heme binding induces dimerization and nitration of truncated beta-amyloid peptide Abeta16 under oxidative stress. *Angew Chem Int Ed Engl* **52**, 8041-8044.
- [29] Galeazzi L, Ronchi P, Franceschi C, Giunta S (1999) In vitro peroxidase oxidation induces stable dimers of beta-amyloid (1-42) through dityrosine bridge formation. *Amyloid* **6**, 7-13.
- [30] Howlett D, Cutler P, Heales S, Camilleri P (1997) Hemin and related porphyrins inhibit beta-amyloid aggregation. *FEBS Lett* **417**, 249-251.
- [31] Liu Y, Carver JA, Ho LH, Elias AK, Musgrave IF, Pukala TL (2014) Hemin as a generic and potent protein misfolding inhibitor. *Biochem Biophys Res Commun* **454**, 295-300.
- [32] Adler J, Scheidt HA, Kruger M, Thomas L, Huster D (2014) Local interactions influence the fibrillation kinetics, structure and dynamics of Abeta(1-40) but leave the general fibril structure unchanged. *Phys Chem Chem Phys* **16**, 7461-7471.
- [33] Zhou Y, Wang J, Liu L, Wang R, Lai X, Xu M (2013) Interaction between amyloid-beta peptide and heme probed by electrochemistry and atomic force microscopy. *ACS Chem Neurosci* **4**, 535-539.
- [34] Salahuddin P, Fatima MT, Abdelhameed AS, Nusrat S, Khan RH (2016) Structure of amyloid oligomers and their mechanisms of toxicities: Targeting amyloid oligomers using novel therapeutic approaches. *Eur J Med Chem* **114**, 41-58.
- [35] Neumann B, Yarman A, Wollenberger U, Scheller F (2014) Characterization of the enhanced peroxidatic activity of amyloid beta peptide-hemin complexes towards neurotransmitters. *Anal Bioanal Chem* **406**, 3359-3364.
- [36] Miller NJ, Rice-Evans CA (1996) Spectrophotometric determination of antioxidant activity. *Redox Rep* **2**, 161-171.
- [37] Yuan C, Yi L, Yang Z, Deng Q, Huang Y, Li H, Gao Z (2012) Amyloid beta-heme peroxidase promoted protein nitrotyrosination: Relevance to widespread protein nitration in Alzheimer's disease. *J Biol Inorg Chem* **17**, 197-207.
- [38] Re R, Pellegrini N, Proteggente A, Pannala A, Yang M, Rice-Evans C (1999) Antioxidant activity applying an improved ABTS radical cation decolorization assay. *Free Radic Biol Med* **26**, 1231-1237.
- [39] Fonteh FA, Grandison AS, Lewis MJ (2002) Variations of lactoperoxidase activity and thiocyanate content in cows' and goats' milk throughout lactation. *J Dairy Res* **69**, 401-409.
- [40] Beers RF, Sizer IW (1952) A spectrophotometric method for measuring the breakdown of hydrogen peroxide by catalase. *J Biol Chem* **195**, 133-140.
- [41] Gau J, Furtmuller PG, Obinger C, Arnhold J, Flemmig J (2015) Enhancing hypothiocyanite production by lactoperoxidase – mechanism and chemical properties of promoters. *Biochim Biophys Reports* **4**, 257-267.
- [42] Dalle-Donne I, Milzani A, Colombo R (2001) Fluorometric detection of dityrosine coupled with HPLC separation for determining actin oxidation. *App Note*, 34-35.
- [43] Flemmig J, Arnhold J (2010) Interaction of hypochlorous acid and myeloperoxidase with phosphatidylserine in the presence of ammonium ions. *J Inorg Biochem* **104**, 759-764.
- [44] LeVine H (1993) Thioflavine T interaction with synthetic Alzheimer's disease beta-amyloid peptides: Detection of amyloid aggregation in solution. *Protein Sci* **2**, 404-410.
- [45] Xue C, Lin TY, Chang D, Guo Z (2017) Thioflavin T as an amyloid dye: Fibril quantification, optimal concentration and effect on aggregation. *R Soc Open Sci* **4**, 1-12.
- [46] Liu IH, Uversky VN, Munishkina LA, Fink AL, Halfter W, Cole GJ (2005) Agrin binds alpha-synuclein and modulates alpha-synuclein fibrillation. *Glycobiology* **15**, 1320-1331.
- [47] Nielsen L, Khurana R, Coats A, Frokjaer S, Brange J, Vyas S, Uversky VN, Fink AL (2001) Effect of environmental factors on the kinetics of insulin fibril formation: Elucidation of the molecular mechanism. *Biochemistry* **40**, 6036-6046.
- [48] Hsiao K, Chapman P, Nilsen S, Eckman C, Harigaya Y, Younkin S, Yang F, Cole G (1996) Correlative memory deficits, Abeta elevation, and amyloid plaques in transgenic mice. *Science* **274**, 99-102.
- [49] Kara F, Dongen ES, Schliebs R, Buchem MA, Groot HJ, Alia A (2012) Monitoring blood flow alterations in the Tg2576 mouse model of Alzheimer's disease by in vivo magnetic resonance angiography at 17.6 T. *Neuroimage* **60**, 958-966.
- [50] Braakman N, Matysik J, van Duinen SG, Verbeek F, Schliebs R, de Groot HJ, Alia A (2006) Longitudinal assessment of Alzheimer's beta-amyloid plaque development in transgenic mice monitored by in vivo magnetic resonance microimaging. *J Magn Reson Imaging* **24**, 530-536.
- [51] Smith MA, Harris PL, Sayre LM, Perry G (1997) Iron accumulation in Alzheimer disease is a source of redox-generated free radicals. *Proc Natl Acad Sci U S A* **94**, 9866-9868.
- [52] Smith MA, Hirai K, Hsiao K, Pappolla MA, Harris PL, Siedlak SL, Tabaton M, Perry G (1998) Amyloid-beta deposition in Alzheimer transgenic mice is associated with oxidative stress. *J Neurochem* **70**, 2212-2215.
- [53] Cullen KM, Kocsi Z, Stone J (2006) Microvascular pathology in the aging human brain: Evidence that senile plaques are sites of microhaemorrhages. *Neurobiol Aging* **27**, 1786-1796.
- [54] Nakagawa K, Kiko T, Miyazawa T, Sookwong P, Tsuduki T, Satoh A, Miyazawa T (2011) Amyloid beta-induced erythrocytic damage and its attenuation by carotenoids. *FEBS Lett* **585**, 1249-1254.
- [55] Dorr A, Sled JG, Kabani N (2007) Three-dimensional cerebral vasculature of the CBA mouse brain: A magnetic resonance imaging and micro computed tomography study. *Neuroimage* **35**, 1409-1423.

- [56] El Tayara NT, Delatour B, Volk A, Dhenain M (2010) Detection of vascular alterations by in vivo magnetic resonance angiography and histology in APP/PS1 mouse model of Alzheimer's disease. *MAGMA* **23**, 53-64.
- [57] Beckmann N, Stirnimann R, Bochen D (1999) High-resolution magnetic resonance angiography of the mouse brain: Application to murine focal cerebral ischemia models. *J Magn Reson* **140**, 442-450.
- [58] Flemmig J, Schlorke D, Kuhne FW, Arnhold J (2016) Inhibition of the heme-induced hemolysis of red blood cells by the chlorite-based drug WF10. *Free Radic Res* **50**, 1386-1395.
- [59] Beaven GH, Chen SH, d'Albis A, Gratzler WB (1974) A spectroscopic study of the haemin-human-serum-albumin system. *Eur J Biochem* **41**, 539-546.
- [60] Kadnikova EN, Kostic NM (2002) Oxidation of ABTS by hydrogen peroxide catalyzed by horseradish peroxidase encapsuled into sol-gel glass. Effects of glass matrix on reactivity. *J Mol Cat B Enzym* **18**, 39-48.
- [61] Khodarahmi R, Ashrafi-Kooshk MR (2017) Is there correlation between Abeta-heme peroxidase activity and the peptide aggregation state? A literature review combined with hypothesis. *Int J Biol Macromol* **100**, 18-36.
- [62] Zschaler J, Dorow J, Schope L, Ceglarek U, Arnhold J (2015) Impact of myeloperoxidase-derived oxidants on the product profile of human 5-lipoxygenase. *Free Radic Biol Med* **85**, 148-156.
- [63] Arnhold J, Flemmig J (2010) Human myeloperoxidase in innate and acquired immunity. *Arch Biochem Biophys* **500**, 92-106.
- [64] Flemmig J, Gau J, Schlorke D, Arnhold J (2016) Lactoperoxidase as a potential drug target. *Expert Opin Ther Targets* **20**, 447-461.
- [65] Azimi S, Rauk A (2013) Fe(III)-heme complexes with the amyloid beta peptide of Alzheimer's disease: QM/MM investigations of binding and redox properties of heme bound to the His residues of Abeta(1-42). *J Chem Theory Comput* **9**, 4233-4242.
- [66] Jayakumar R, Kusiak JW, Chrest FJ, Demehin AA, Murali J, Wersto RP, Nagababu E, Ravi L, Rifkind JM (2003) Red cell perturbations by amyloid beta-protein. *Biochim Biophys Acta* **1622**, 20-28.
- [67] Ravi LB, Poosala S, Ahn D, Chrest FJ, Spangler EL, Jayakumar R, Nagababu E, Mohanty JG, Talan M, Ingram DK, Rifkind JM (2005) Red cell interactions with amyloid-beta(1-40) fibrils in a murine model. *Neurobiol Dis* **19**, 28-37.
- [68] Buss L, Fisher E, Hardy J, Nizetic D, Groet J, Pulford L, Strydom A (2016) Intracerebral haemorrhage in Down syndrome: Protected or predisposed? *FL1000Res* **5**, 1-12.
- [69] Forman HJ, Bernardo J, Davies KJA (2016) What is the concentration of hydrogen peroxide in blood and plasma? *Arch Biochem Biophys* **603**, 48-53.
- [70] Brewitz HH, Goradia N, Schubert E, Galler K, Kuhl T, Syllwasschy B, Popp J, Neugebauer U, Hagelueken G, Schiemann O, Ohlenschlager O, Imhof D (2016) Heme interacts with histidine- and tyrosine-based protein motifs and inhibits enzymatic activity of chloramphenicol acetyltransferase from Escherichia coli. *Biochim Biophys Acta* **1860**, 1343-1353.
- [71] Marquez LA, Dunford HB (1995) Kinetics of oxidation of tyrosine and dityrosine by myeloperoxidase compounds I and II. Implications for lipoprotein peroxidation studies. *J Biol Chem* **270**, 30434-30440.
- [72] Nomura K, Suzuki N, Matsumoto S (1990) Pulcherosine, a novel tyrosine-derived, trivalent cross-linking amino acid from the fertilization envelope of sea urchin embryo. *Biochemistry* **29**, 4525-4534.
- [73] Heinecke JW, Li W, Daehne HL, Goldstein JA (1993) Dityrosine, a specific marker of oxidation, is synthesized by the myeloperoxidase-hydrogen peroxide system of human neutrophils and macrophages. *J Biol Chem* **268**, 4069-4077.
- [74] Gunn AP, Wong BX, Johanssen T, Griffith JC, Masters CL, Bush AI, Barnham KJ, Duce JA, Cherny RA (2016) Amyloid-beta peptide Abeta3pE-42 induces lipid peroxidation, membrane permeabilization, and calcium influx in neurons. *J Biol Chem* **291**, 6134-6145.
- [75] Bao Q, Luo Y, Li W, Sun X, Zhu C, Li P, Huang ZX, Tan X (2011) The mechanism for heme to prevent Abeta(1-40) aggregation and its cytotoxicity. *J Biol Inorg Chem* **16**, 809-816.
- [76] Tycko R (2016) Molecular structure of aggregated Amyloid-beta: Insights from solid-state nuclear magnetic resonance. *Cold Spring Harb Perspect Med* **6**, 1-22.
- [77] Tran L, Ha-Duong T (2015) Exploring the Alzheimer amyloid-beta peptide conformational ensemble: A review of molecular dynamics approaches. *Peptides* **69**, 86-91.
- [78] Atamna H (2009) Amino acids variations in amyloid-beta peptides, mitochondrial dysfunction, and new therapies for Alzheimer's disease. *J Bioenerg Biomembr* **41**, 457-464.
- [79] Yu HL, Chertkow HM, Bergman H, Schipper HM (2003) Aberrant profiles of native and oxidized glycoproteins in Alzheimer plasma. *Proteomics* **3**, 2240-2248.
- [80] Sung HY, Choi BO, Jeong JH, Kong KA, Hwang J, Ahn JH (2016) Amyloid beta-mediated hypomethylation of heme oxygenase 1 correlates with cognitive impairment in Alzheimer's disease. *PLoS One* **11**, e0153156.
- [81] Gupta A, Lacoste B, Pistell PJ, Ingram DK, Hamel E, Alaoui-Jamali MA, Szarek WA, Vlahakis JZ, Jie S, Song W, Schipper HM (2014) Neurotherapeutic effects of novel HO-1 inhibitors in vitro and in a transgenic mouse model of Alzheimer's disease. *J Neurochem* **131**, 778-790.
- [82] Slemmon JR, Hughes CM, Campbell GA, Flood DG (1994) Increased levels of hemoglobin-derived and other peptides in Alzheimer's disease cerebellum. *J Neurosci* **14**, 2225-2235.
- [83] Kiko T, Nakagawa K, Satoh A, Tsuduki T, Furukawa K, Arai H, Miyazawa T (2012) Amyloid beta levels in human red blood cells. *PLoS One* **7**, e49620.
- [84] Gilca M, Lixandru D, Gaman L, Virgolici B, Atanasiu V, Stoian I (2014) Erythrocyte membrane stability to hydrogen peroxide is decreased in Alzheimer disease. *Alzheimer Dis Assoc Disord* **28**, 358-363.
- [85] Habib LK, Lee MT, Yang J (2010) Inhibitors of catalase-amyloid interactions protect cells from beta-amyloid-induced oxidative stress and toxicity. *J Biol Chem* **285**, 38933-38943.
- [86] Nakagawa K, Kiko T, Kuriwada S, Miyazawa T, Kimura F, Miyazawa T (2011) Amyloid beta induces adhesion of erythrocytes to endothelial cells and affects endothelial viability and functionality. *Biosci Biotechnol Biochem* **75**, 2030-2033.
- [87] Ravi LB, Mohanty JG, Chrest FJ, Jayakumar R, Nagababu E, Usatyuk PV, Natarajan V, Rifkind JM (2004) Influence of beta-amyloid fibrils on the interactions between red blood cells and endothelial cells. *Neurol Res* **26**, 579-585.

- [88] Schmaier AH (2016) Alzheimer's disease is in-part a thrombo-hemorrhagic disorder. *J Thromb Haemost* **14**, 1-4.
- [89] Everse J, Coates PW (2009) Neurodegeneration and peroxidases. *Neurobiol Aging* **30**, 1011-1025.
- [90] Kato Y, Maruyama W, Naoi M, Hashizume Y, Osawa T (1998) Immunohistochemical detection of dityrosine in lipofuscin pigments in the aged human brain. *FEBS Lett* **439**, 231-234.
- [91] Pirolta V, Monzani E, Dell'Acqua S, Casella L (2016) Interactions between heme and tau-derived R1 peptides: Binding and oxidative reactivity. *Dalton Trans* **45**, 14343-14351.
- [92] Brier MR, Gordon B, Friedrichsen K, McCarthy J, Stern A, Christensen J, Owen C, Aldea P, Su Y, Hassenstab J, Cairns NJ, Holtzman DM, Fagan AM, Morris JC, Benzinger TL, Ances BM (2016) Tau and Abeta imaging, CSF measures, and cognition in Alzheimer's disease. *Sci Transl Med* **8**, 1-19.